

**Insight into PM<sub>2.5</sub> Sources by Applying Positive  
Matrix Factorization (PMF) at an Urban and  
Rural Site of Beijing**

**Deepchandra Srivastava<sup>1</sup>, Jingsha Xu<sup>1</sup>, Tuan V. Vu<sup>1,2</sup>  
Di Liu<sup>1,3</sup>, Linjie Li<sup>3</sup>, Pingqing Fu<sup>4</sup>, Siqi Hou<sup>1</sup>, Zongbo Shi<sup>1,\*</sup>  
and Roy M. Harrison<sup>1†\*</sup>**

**<sup>1</sup> School of Geography Earth and Environmental Science, University  
of Birmingham, Birmingham, B15 2TT  
United Kingdom**

**<sup>2</sup> Now at: School of Public Health, Imperial College London, London  
United Kingdom**

**<sup>3</sup> Institute of Atmospheric Physics, Chinese Academy of Sciences  
Beijing, 100029, China**

**<sup>4</sup> Institute of Surface-Earth System Science, Tianjin University,  
Tianjin 300072, China**

**† Also at: Department of Environmental Sciences / Centre of Excellence in Environmental  
Studies, King Abdulaziz University, PO Box 80203, Jeddah, 21589, Saudi Arabia**

**Corresponding author: E-mail: [r.m.harrison@bham.ac.uk](mailto:r.m.harrison@bham.ac.uk) (Roy M. Harrison) and  
[z.shi@bham.ac.uk](mailto:z.shi@bham.ac.uk) (Zongbo Shi)**

## 31 ABSTRACT

32 This study presents the source apportionment of PM<sub>2.5</sub> performed by PMF on data collected at an  
33 urban (Institute of Atmospheric Physics - IAP) and a rural site (Pinggu-PG) in Beijing as part of the  
34 Atmospheric Pollution and Human Health in a Chinese megacity (APHH-Beijing) field campaigns.  
35 The campaigns were carried out from 9<sup>th</sup> November to 11<sup>th</sup> December 2016 and 22<sup>nd</sup> May to 24<sup>th</sup> June  
36 2017. The PMF included both organic and inorganic species, and a seven-factor output provided the  
37 most reasonable solution for the PM<sub>2.5</sub> source apportionment. These factors are interpreted to be  
38 traffic emissions, biomass burning, road dust, soil dust, coal combustion, oil combustion and  
39 secondary inorganics. Major contributors to PM<sub>2.5</sub> mass were secondary inorganics (IAP: 22%; PG:  
40 24%), biomass burning (IAP: 36%; PG: 30%), and coal combustion (IAP: 20%; PG: 21%) sources  
41 during the winter period at both sites. Secondary inorganics (48%), road dust (20%) and coal  
42 combustion (17%) showed the highest contribution during summer at PG, while PM<sub>2.5</sub> particles were  
43 mainly composed of soil dust (35%) and secondary inorganics (40%) at IAP. Despite this, factors that  
44 were resolved based on metal signatures were not fully resolved and indicate a mixing of two or more  
45 sources. PMF results were also compared with sources resolved from another receptor model (i.e.  
46 CMB) and PMF performed on other measurements (i.e. online and offline aerosol mass spectrometry  
47 (AMS)) and showed a good agreement for some but not all sources. The biomass burning factor in  
48 PMF may contain aged aerosols as a good correlation was observed between biomass burning and  
49 oxygenated fractions ( $r^2=0.6-0.7$ ) from AMS. The PMF failed to resolve some sources identified by  
50 the CMB and AMS, and appears to overestimate the dust sources. A comparison with earlier PMF  
51 source apportionment studies from the Beijing area highlights the very divergent findings from  
52 application of this method.

53 **Key words:** Source apportionment; PM<sub>2.5</sub>; Beijing; PMF; CMB; online AMS; offline AMS

54

## 55 1. INTRODUCTION

56 Atmospheric particulate matter (PM) is composed of various chemical components and can affect air  
57 quality (and consequently human health), visibility, and ecosystems (Boucher et al., 2013; Heal et al.,  
58 2012). Through absorption and scattering of solar radiation and by affecting clouds, PM also have a  
59 major impact on the climate, and thus the hydrological cycle. PM with an aerodynamic diameter less  
60 than 2.5  $\mu\text{m}$  ( $\text{PM}_{2.5}$ ) is given special attention due to its adverse effects on human health as it can  
61 penetrate deep into human lungs when inhaled. Several recent studies have indicated that many  
62 adverse health outcomes, such as respiratory and cardiovascular morbidity and mortality, are related  
63 to long-term exposure to PM (Lu et al., 2021; Wang et al., 2016; Xing et al., 2016; Xie et al., 2019).  
64 In addition, over a million premature deaths per year are reported in China due to poor air quality  
65 (GBD MAPS Working Group, 2016). Beijing, the capital city of China, is a megacity with  
66 approximately 21 million inhabitants that are regularly exposed to severe haze events. For example,  
67 77 pollution episodes (defined as two or more consecutive days where the average  $\text{PM}_{2.5}$   
68 concentration exceeds  $75 \mu\text{g m}^{-3}$ ) were observed between April 2013 to March 2015 (Batterman et  
69 al., 2016).  $\text{PM}_{2.5}$  concentrations have reached  $1,000 \mu\text{g m}^{-3}$  in some heavily polluted areas of Beijing  
70 (Ji et al., 2014). In addition, a study compared the number of cases of acute cardiovascular,  
71 cerebrovascular, and respiratory diseases in the Beijing Emergency Center and haze data from Beijing  
72 Observatory between 2006 and 2013. Their results showed a rising trend, highlighting the average  
73 number of cases per day for all three diseases was higher on hazy days than on non-hazy days (Zhang  
74 et al., 2015). Therefore, major control measures were implemented to reduce  $\text{PM}_{2.5}$  pollution in  
75 Beijing (Vu et al., 2019). Recently, one-third of Chinese cities in 2020 were kept under lockdown to  
76 prevent the transmission of COVID-19 virus, which strictly curtailed personal mobility and economic  
77 activities. The lockdown led to an improvement in air quality and managed to bring down the levels  
78 of  $\text{PM}_{2.5}$ . Despite these improvements,  $\text{PM}_{2.5}$  concentrations during the lockdown periods remained  
79 higher than the World Health Organization recommendations, suggesting much further effort is

needed (He et al., 2020; Le et al., 2020; Shi et al., 2021). A quantitative source apportionment provides key information to support such efforts.

Receptor models are widely used for source apportionment of PM<sub>2.5</sub>. These methods include positive matrix factorization (PMF) (Paatero, 1997; Paatero and Tapper, 1994), principal component analysis (PCA) (Lee et al., 2011), chemical mass balance (CMB) (Watson et al., 1990), and UNMIX (Herrera Murillo et al., 2012). Among these methods, PMF is a widely used multivariate method that can resolve the dominant positive factors without prior knowledge of sources. Previous PMF studies, based on high resolution Aerosol Mass Spectrometer data, have provided valuable information on the sources of PM in urban Beijing and its surrounding areas (Zhang et al., 2015; Huang et al., 2010; Sun et al., 2010; Sun et al., 2013; Zhang et al., 2013; Zhang et al., 2014; Zhang et al., 2017; Zhang et al., 2016; Hu et al., 2016; Qiu et al., 2019). However, the factors that influence haze formation and related sources remain unclear due to its inherent complexity (Tie et al., 2017; Sun et al., 2014). Filter-based PMF studies provide a valuable tool for identifying sources of airborne particles, by utilising size-resolved chemical information (Li et al., 2019; Ma et al., 2017a; Tian et al., 2016; Yu et al., 2013; Song et al., 2007; Song et al., 2006). These source apportionment studies have predominantly used OC (organic carbon), EC (elemental carbon), water soluble ions and metals as the input data matrix to explore the co-variances between species and their associated sources, but to the best of our knowledge, the use of organic markers in PMF has not been explored extensively in Beijing. The use of organic molecular markers in PMF has enhanced our understanding of the PM fraction as they can be source specific (Shrivastava et al., 2007; Jaekels et al., 2007; Zhang et al., 2009; Wang et al., 2012; Srimuruganandam and Shiva Nagendra, 2012; Schembari et al., 2014; Laing et al., 2015; Waked et al., 2014; Srivastava et al., 2018) and could potentially offer a clearer link between factors and sources.

105 This study presents the results obtained from the PMF model applied to a filter-based dataset collected  
106 in the Beijing metropolitan area at two sites, urban and rural. The study provides source  
107 apportionment results from both urban and rural locations in Beijing including their temporal and  
108 spatial variations. In addition, the study also presents a short summary of previously published filter-  
109 based studies conducted in the Beijing metropolitan area and their major outcomes. A comparison of  
110 the present PMF results was also made with other source apportionment approaches or applications  
111 of PMF to other datasets, with an aim to discuss the existing PM sources in the Beijing metropolitan  
112 area, including focusing on the strengths and weaknesses of the source apportionment approach  
113 employed.

114

## 115 **2. METHODOLOGY**

116 Details about the sampling site, measurements, sample collection and analytical procedures are  
117 reported elsewhere (Shi et al., 2019; Xu et al., 2021; Wu et al., 2020), and hence only the essential  
118 information is presented in this section.

119

### 120 **2.1 Sampling Site and Sample Collection**

121 The PM<sub>2.5</sub> sampling was conducted simultaneously at the urban and rural sites from 9<sup>th</sup> November to  
122 12<sup>th</sup> December 2016 and 22<sup>nd</sup> May to 24<sup>th</sup> June 2017 as part of the Atmospheric Pollution and Human  
123 Health in a Chinese megacity (APHH-Beijing) field campaigns (Shi et al., 2019) (Figure S1). The  
124 urban sampling site (116.39E, 39.98N) - the Institute of Atmospheric Physics (IAP) of the Chinese  
125 Academy of Sciences in Beijing, represents typical condition of central Beijing, there are various  
126 roads nearby including a highway road approximately 200 m away. The rural Pinggu site (PG)  
127 (40.17N, 117.05E) is located in Xibaidian village. This site is approximately 60 km to the north-east  
128 of Beijing city centre and about 4 km north-west of the Pinggu town centre. The site is surrounded

129 by trees and farmland. In addition, residents mainly use coal and biomass for heating and cooking in  
130 individual homes.

131

132 24-hour PM<sub>2.5</sub> samples were collected every day on pre-baked quartz filters (Pallflex, 8×10 inch) and  
133 47 mm PTFE filters (flow rate of 15.0 L min<sup>-1</sup>) using high volume (Tisch, USA, flow rate of 1.1 m<sup>3</sup>  
134 min<sup>-1</sup>) and medium volume (Thermo Scientific Partisol 2025i) air sampler. Field blanks were also  
135 collected during the sampling campaign at both sites. The quartz filters were then analyzed for organic  
136 tracers, OC/EC and ion species. PTFE filters were used for the determination of PM<sub>2.5</sub> mass and  
137 metals. Details on preparation and conservation of these filter samples have already been reported  
138 elsewhere (Wu et al., 2020; Xu et al., 2021).

139

140 Real time composition of non-refractory PM<sub>1</sub> particles (NR-PM<sub>1</sub>) was measured using an Aerodyne  
141 aerosol mass spectrometer (AMS) at a time resolution of 2.5 min. The operational details on the AMS  
142 measurements have been given elsewhere (Xu et al., 2019). In addition, the measurements of gaseous  
143 species such as O<sub>3</sub>, CO, NO, NO<sub>2</sub> and SO<sub>2</sub> were performed using gas analyzers. The meteorological  
144 parameters including temperature (T), relative humidity (RH), wind speed (WS), and wind direction  
145 (WD) were also measured at both sites.

146

## 147 **2.2 Analytical Procedure**

148 In all 62 and 72 chemical species were quantified in each PM<sub>2.5</sub> sample from IAP and PG,  
149 respectively. This included EC/ OC, 36 organic tracers, 7 major inorganic ions (Na<sup>+</sup>, K<sup>+</sup>, Ca<sup>2+</sup>, NH<sub>4</sub><sup>+</sup>,  
150 Cl<sup>-</sup>, NO<sub>3</sub><sup>-</sup> and SO<sub>4</sub><sup>2-</sup>) and 17 metallic elements (V, Cr, Co, Mn, Ni, Cu, Zn, As, Br, Sr, Ag, Cd, Sn,  
151 Sb, Ba, Hg and Pb) at IAP. Similarly, the identified species at PG included EC/OC, 51 organic tracers,  
152 7 major inorganic ions and 12 metallic elements (V, Cr, Co, Mn, Ni, Cu, Zn, As, Sr, Sb, Ba, and Pb).  
153 EC and OC measurements were performed using a Sunset lab analyser (model RT-4) and DRI multi-

154 wavelength thermal-optical carbon (model 2015) analyser based on the EUSAAR2 (European  
155 Supersites for Atmospheric Aerosol Research) transmittance protocol at both sites, IAP and PG,  
156 respectively, following the procedure explained by Paraskevopoulou et al. (2014). Major inorganic  
157 ions and metallic elements were analysed using an ion chromatograph (Dionex, Sunnyvale, CA,  
158 USA) and Inductively coupled plasma-mass spectrometer (ICP-MS) at both sites, respectively. Major  
159 crustal elements including Al, Si, Ca, Ti and Fe were determined by X-ray fluorescence spectrometer  
160 (XRF).

161  
162 Organic tracers at IAP included n-alkanes 11 C<sub>24</sub>-C<sub>34</sub>, 2 hopanes, 17 PAHs, 3 anhydrous sugars  
163 (levoglucosan, mannosan, galactosan), 2 fatty acids (palmitic acid, stearic acid) and cholesterol.  
164 These organic tracers were analysed by gas chromatography mass spectrometry (GC/MS, Agilent  
165 7890A GC plus 5975C mass-selective detector) coupled with a DB-5MS column (30 m × 0.25 mm ×  
166 0.25 µm) following the protocol explained in Xu et al. (2020). At PG, organic tracers were analysed  
167 based on the method reported by Wu et al. (2020) using GC/MS (Agilent GC-6890N plus MSD-  
168 5973N) coupled with a HP-5MS column (30 m × 0.25 mm × 0.25 µm). This included quantification  
169 of similar species (12 n-alkanes C<sub>24</sub>-C<sub>35</sub>, 9 hopanes, 22 PAHs, 3 anhydrous sugars (levoglucosan,  
170 mannosan, galactosan), 4 fatty acids (palmitic acid, stearic acid, linoleic acid, oleic acid) and  
171 cholesterol) with few additional ones. Recoveries for the identified organic tracers ranged from 70-  
172 100% and 80-110 %, at IAP and PG, respectively. Field blank were also analysed as part of quality  
173 control and demonstrated very low contamination (<5%).

174  
175 In addition, one or two punches of PM<sub>2.5</sub> filter sample were also analysed offline using AMS to  
176 investigate the water-soluble OA (WSOA) mass spectra following the procedure explained  
177 previously (Qiu et al., 2019).

178

## 179 2.4 Positive Matrix Factorization

180 Detailed information on the receptor modelling methods used within this study can be found  
 181 elsewhere (Paatero and Tapper, 1994; Hopke, 2016). Positive matrix factorization (PMF) is a  
 182 multivariate factor analysis tool and based on a weighted least square fit, where the weights are  
 183 derived from the analytical uncertainty. The best model solution was obtained by minimizing  
 184 residuals obtained between modeled and observed input species concentrations Estimation of  
 185 analytical uncertainties for the filter-based measurements was calculated using Eq. (1) (Polissar et al.,  
 186 1998).

$$187 \quad \sigma_{ij} = \begin{cases} \frac{5}{6}LD_j & \text{if } X_{ij} < LD_j \\ \sqrt{(0.5 * LD_j)^2 + (EF_j X_{ij})^2} & \text{if } X_{ij} \geq LD_j \end{cases} \quad \text{Eq. (1)} \quad 188$$

189 where  $LD_j$  is the detection limit for compound  $j$  and  $EF_j$  is the error fraction for the compound  $j$ . The  
 190 detection limits of all compounds used in the PMF model is given in Table S1 (SI). The U.S.  
 191 Environmental Protection Agency (US-EPA) PMF 5.0 software was used in this work to perform the  
 192 source apportionment.  
 193

194 ***Selection of the input data.*** The selection of species used as input data for the PMF analysis is  
 195 important and can significantly influence the model results (Lim et al., 2010). The following set of  
 196 criteria were used for the selection of the input species: signal to noise ratio (S/N) (Paatero and Hopke,  
 197 2003), major PM chemical species, compounds with maximum data points above the detection limit  
 198 and those being considered as specific markers of a given source (e.g., levoglucosan, picene) (Oros  
 199 and Simoneit, 2000; Simoneit, 1999) were selected. These steps were taken to limit the input data  
 200 matrix according to the total number of samples (n=133); some species were also not included if they  
 201 belonged to a single source and correlated with another marker of this source. A total of 31 species  
 202 were used in the model ( $PM_{2.5}$ , OC, EC,  $K^+$ ,  $Na^+$ ,  $Ca^{2+}$ ,  $NH_4^+$ ,  $NO_3^-$ ,  $SO_4^{2-}$ ,  $Cl^-$ , Ti, V, Mn, Ni, Zn, Pb,  
 203



204 Cu, Fe, Al, C26, C29, C31, 17 $\alpha$ (H)-22,29,30-trisnorhopane, 17 $\beta$ (H), 21 $\alpha$ (H)-30-norhopane, chrysene,  
205 benzo(b)fluoranthene, benzo(a)pyrene, picene, corene, levoglucosan, and stearic acid). The  
206 concentration of PM<sub>2.5</sub> was included as a total variable in the model (with large uncertainties) to  
207 directly determine the source contributions to the daily mass concentrations.

208  
209 ***Selection of the final solution.*** As normally recommended, a detailed evaluation of factor profiles,  
210 temporal trends, fractional contribution of major species to each factor and correlations with external  
211 tracers, were investigated carefully to select the appropriate number of factors.

212  
213 A few constraints were also applied to the base run to obtain clearer chemical source profiles in the  
214 final solution. The general framework for applying constraints to PMF solutions has already been  
215 discussed elsewhere (Amato et al., 2009; Amato and Hopke, 2012). The changes in the  $Q$  values were  
216 considered here as a diagnostic parameter to provide insight into the rotation of factors. All model  
217 runs were carefully monitored by examining the  $Q$  values obtained in the robust mode. To limit  
218 change in the  $Q$ -value, only “soft pulling” constraints were applied. The change in the  $Q$ -robust was  
219  $< 1\%$ , which is acceptable as per PMF guidelines ( $< 5\%$ ) (Norris et al., 2014). Finally, three criteria  
220 were used to select the optimal solution, including correlation coefficient ( $r$ ) between the measured  
221 and modelled species, bootstrap and t-test (two-tailed paired t-test) performed on the base and  
222 constraint runs, as explained previously (Srivastava et al., 2018).

223

## 224 **2.5 Back trajectories and Geographical Origins**

225 The geographical origin of selected identified sources and pollutants was investigated using  
226 concentration-weighted trajectory (CWT), non-parametric wind regression (NWR), and cluster  
227 analysis methods. NWR combines ambient concentrations with co-located measurements of wind  
228 direction and speed and highlights wind sectors that are associated with high measured concentrations  
229 (Henry et al., 2009). The general principle is to smooth the data over a fine grid, so that a weighted

concentration could be estimated by any wind direction ( $\phi$ )/wind speed ( $v$ ) couple, where the weighing coefficients are determined through Gaussian-like functions. CWT and cluster analysis assess the potential transport of pollution over large geographical scale (Polissar et al., 2001). These approaches combine atmospheric concentrations measured at the receptor site with back trajectories and residence time information and help to geographically evaluate air parcels responsible for high concentrations. For this purpose, hourly 24-h back trajectories arriving at 200 m above sea level were calculated from the PC-based version of HYSPLIT v4.1 (Stein et al., 2015; Draxler, 1999). NWR, CWT calculations and cluster analysis, were performed using the ZeFir Igor package (Petit et al., 2017).

239

## 240 **2.6 Other Receptor Modelling Approaches**

Sources were also resolved at both sites separately using another receptor model known as chemical mass balance (CMB) as well as PMF performed on high resolution AMS data collected at IAP. Details on sources resolved using these approaches are reported elsewhere (Wu et al., 2020; Xu et al., 2021; Sun et al., 2020).

245

Briefly, CMB is based on a linear least squares approach and accounts for uncertainties in both, source profiles and ambient measurements to apportion the sources of OC. The US EPA CMB8.2 software was used for this purpose at both sites. The source profiles applied in the model were taken from local studies to better represent the sources, including profiles of straw burning (Zhang et al., 2007), wood burning (Wang et al. 2009), gasoline and diesel vehicles (Cai et al. 2017), industrial and residential coal combustion (Zhang et al., 2008), and cooking (Zhao et al., 2015). Only the source profile for vegetative detritus (Rogge et al. 1993; Wang et al., 2009) was not available from local studies. The selected fitting species included EC, anhydrous sugar (levoglucosan), fatty acids, PAHs, hopanes and alkanes

### 255 3. RESULTS AND DISCUSSION

#### 256 3.1 Overview on PM Sources in Beijing based on the Current Source Apportionment Study

257 A seven-factor output provided the most reasonable solution for the PM<sub>2.5</sub> source apportionment  
258 performed on the combined dataset from IAP and PG (Figures 1 and 2).

259

260 Based on the factor profiles, we identified traffic emissions, biomass burning, road dust, soil dust,  
261 coal combustion, oil combustion and secondary inorganics. For the same dataset, solutions with six  
262 sources were less explanatory and some factors were mixed. Conversely, an increase in the number  
263 of factors led to the split of meaningful factor profiles. In the final solution, the comparison of the  
264 reconstructed PM<sub>2.5</sub> contributions from all sources with measured PM<sub>2.5</sub> concentrations for different  
265 seasons at both sites showed good mass closure ( $r^2 = 0.61-0.91$ , slope = 0.99-1.12,  $p < 0.05$ , ODR  
266 (orthogonal distance regression)). A low  $r^2$  (0.61) value was observed for the summer period at IAP  
267 (Figure S2). This may be due to the inability of PMF to model low concentrations observed for  
268 sources such as biomass burning and coal combustion during the summer. In addition, most of the  
269 species showed good agreement with measured concentrations (Table S2). Bootstrapping on the final  
270 solution showed stable results with more than 95 out of 100 bootstrap mapped factors (Table S3).  
271 Finally, no significant difference ( $p > 0.05$ ) was observed in the factor chemical profiles between the  
272 base and the constrained runs (Table S4).

273

274 Overall, secondary inorganics, biomass burning, and coal combustion sources were the main  
275 contributors to the total PM<sub>2.5</sub> mass during winter (Figure 3). These sources accounted for 22%, 36%,  
276 20%, and 24%, 30%, 21% of PM<sub>2.5</sub> mass at IAP and PG, respectively. Secondary inorganics, road  
277 dust and coal combustion showed the highest contribution during summer at PG, while PM<sub>2.5</sub> particles  
278 were mainly composed of soil dust and secondary inorganics at IAP. Identified aerosol sources, factor  
279 profiles and temporal evolutions are discussed below. Note, PMF was carried out on the combined  
280 datasets and thus only provides a single set of factor profiles for both sites. Similar to previous studies

281 (Li et al., 2019; Ma et al., 2017a; Tian et al., 2016; Yu et al., 2013; Liu et al., 2019; Zhang et al.,  
282 2013), neither secondary organic aerosol nor cooking emissions were identified, and given the good  
283 mass closure must be present within other source categories.

284  
285 **Coal combustion.** Coal combustion was identified based on it accounting for a high proportion of  
286 PAHs (27-78%), especially picene (78%) as a specific marker of coal combustion (Oros and  
287 Simoneit, 2000), together with significant amount of OC (45%) and EC (29%) (Figure 1). This factor  
288 also made a substantial contribution to n-alkanes (28-58%), stearic acid (64%) and hopanes (53-56%),  
289 as these compounds are also abundant in coal smoke (Bi et al., 2008; Zhang et al., 2008; Oros and  
290 Simoneit, 2000; Guo et al., 2015).

291  
292 The coal combustion factor accounted for 20% of the PM mass ( $16.0 \mu\text{g m}^{-3}$ ) at the urban site IAP  
293 during winter and followed typical seasonal variations. However, the contributions of this source to  
294  $\text{PM}_{2.5}$  mass were broadly similar (21% vs 17%, Figure 3) at PG during both seasons, while the average  
295 concentrations were higher in winter than summer ( $19.4 \mu\text{g m}^{-3} > 4.6 \mu\text{g m}^{-3}$ ). Due to a lack of  
296 infrastructure at the rural site PG, the residents still use coal for cooking and heating purposes at the  
297 time of sampling (Shi et al., 2019). There is a reduction in coal usage for heating due to elevated  
298 temperatures in the summertime, leading to low levels of this factor. But the similar contribution at  
299 the rural site could be linked to consistent cooking activities throughout the year (Figure 2) (Shi et  
300 al., 2019; Tao et al., 2018). These results were in good agreement with previous observations reported  
301 at the same urban site (18%) (Ma et al., 2017a; Tian et al., 2016). In addition, similar contributions  
302 were also observed at other urban locations around Beijing (Wang et al., 2008; Liu et al., 2019).

303  
304 This factor also included significant contributions from levoglucosan (60%). Levoglucosan, a major  
305 pyrolysis product of cellulose, and has been proposed as molecular marker of biomass burning  
306 aerosols (Simoneit, 1999). A study conducted in China suggested that residential coal combustion  
307 can also contribute significantly to levoglucosan emissions, based on both source testing and ambient

308 measurements (Yan et al., 2018). Therefore, it is expected that the contribution of levoglucosan is  
309 probably linked to residential coal use for cooking in this case. It is also possible that the high  
310 contribution of levoglucosan could also be linked to model bias as the PMF model only provides an  
311 average factor profiles for both sites irrespective of their nature (rural vs. urban) and different  
312 sampling periods (summer vs. winter).

313  
314 This was further supported as NWR and CWT analysis showed similar results, mostly dominated by  
315 a northerly flow during the winter period at both sites. High concentrations of this source and  
316 levoglucosan were observed at low wind speeds (Figure S3), indicating the significant role of local  
317 activities. Higher levels were observed at the rural site PG ( $19.4 \mu\text{g m}^{-3}$  vs  $16.0 \mu\text{g m}^{-3}$  at the urban  
318 site). However, a south-westerly flow was dominant during summer and could be related to transport  
319 of air masses from the Hebei province where a large number of industries operate.

320  
321 **Oil combustion.** The oil combustion factor profile included high contributions to V (79%) and Ni  
322 (70%) (see Figure 1). V and Ni are widely used markers for oil combustion in residential, commercial  
323 and industrial applications (Viana et al., 2008; Mazzei et al., 2008; Pant et al., 2015; Huang et al.,  
324 2021). The V/Ni ratio obtained in this study was 0.9, close to the previously obtained ratio for residual  
325 oil used in power plants (Swietlicki and Krejci, 1996). Results suggest this source might be attributed  
326 to residual oil combustion linked to industrial activities as a large number of highly polluting  
327 industries are still located in the Beijing neighbourhood (Li et al., 2019). CWT and NWR analysis  
328 suggested the influence of regional transport at both sites, highlighting the dominance of south  
329 westerly and south easterly flows during the winter and summer at both sites (Figure S4).

330  
331 The source did not show any seasonal pattern (Figure 2), and accounted for 2% ( $1.4 \mu\text{g m}^{-3}$ ) and 6%  
332 ( $1.6 \mu\text{g m}^{-3}$ ) at IAP, and 8% ( $7.1 \mu\text{g m}^{-3}$ ) and 9% ( $2.1 \mu\text{g m}^{-3}$ ) at PG of the  $\text{PM}_{2.5}$  mass during winter  
333 and summer, respectively (Figure 3). The contribution of this source to the PM mass was within the

334 similar range to the previous study conducted at the same urban site (contribution 4.7%) (Li et al.,  
335 2019), which also found a high proportion of V attributed to the identified source.

336  
337 **Biomass burning.** The biomass burning factor was characterized by high contributions to  $\text{Cl}^-$  (74%),  
338  $\text{K}^+$  (27%) and levoglucosan (25%) (Figure 1). This factor also made significant contributions to PAHs  
339 (Chry (66%), B[b]F (66%), Cor (68%)) and followed a clear seasonal variation with a higher  
340 contribution in winter (Figure 2). It accounted for 36 % ( $29.0 \mu\text{g m}^{-3}$ ) and 30% ( $27.3 \mu\text{g m}^{-3}$ ) of the  
341  $\text{PM}_{2.5}$  mass during the wintertime at IAP and PG, respectively (Figure 3), while the contribution  
342 during the summertime was extremely low. This was expected due to elevated temperature during  
343 the summer period and reduction in biomass burning activities. In addition,  $\text{NO}_3^-$  (24%), and  $\text{NH}_4^+$   
344 (24%) also contributed significantly to the biomass burning factor. Biomass burning is an important  
345 natural source of  $\text{NH}_3$  (Zhou et al., 2020) which rapidly reacts with  $\text{HNO}_3$  to form  $\text{NH}_4\text{NO}_3$  aerosols.  
346 The presence of  $\text{NH}_4\text{NO}_3$  aerosols in biomass burning plumes, has also been reported previously  
347 (Paulot et al., 2017; Zhao et al., 2020).

348  
349 It was unexpected to observe a low contribution of levoglucosan, a known biomass burning marker,  
350 to this factor. However, model bias and the contribution of other relevant sources to levoglucosan  
351 could cause such observations, as discussed above.  $\text{K}^+$  is also produced from the combustion of wood  
352 lignin and has been used extensively as an inorganic tracer to apportion biomass burning contributions  
353 to ambient aerosol (Zhang et al., 2010; Lee et al., 2008a). However, the contribution of  $\text{K}^+$  to this  
354 factor was relatively low, possibly because  $\text{K}^+$  has also other sources, such as soil dust (Duvall et al.,  
355 2008).  $\text{Cl}^-$  can be emitted from both coal combustion and biomass burning, especially during the cold  
356 period in Beijing (Sun et al., 2006). It is also important to note that high  $\text{Cl}^-$  levels observed in this  
357 factor could be associated with coal combustion as  $\text{Cl}^-$  has been used to represent coal combustion  
358 activities in China (Wang et al., 2008). If we consider this, high  $\text{Cl}^-$  levels related to the coal  
359 combustion factor should have also shown a significant contribution to PM mass during the

summertime at the rural site (PG) as residents near the rural site mostly use coal and biomass for cooking activities as discussed above, but they do not. Results suggest this factor can be attributed mainly to biomass burning aerosols in the Beijing metropolitan area, but some influence of coal combustion signals cannot be ignored. Back trajectory analysis also confirmed the local origin of this source during the wintertime at both sites (Figure S5).

The source contribution reported in the present study was higher than that found in earlier studies in Beijing (11-20%) (Li et al., 2019; Ma et al., 2017a; Tian et al., 2016; Yu et al., 2013; Song et al., 2007; Song et al., 2006; Liu et al., 2019), suggesting some inclusion of coal burning. As both these sources follow a similar typical seasonal variation, i.e., high concentration during the cold period, it makes their separation difficult due to correlation.

**Secondary inorganics.** Secondary inorganics were typically characterized by high contributions to  $\text{NO}_3^-$ ,  $\text{SO}_4^{2-}$  and  $\text{NH}_4^+$  (55%, 56% and 56% of the total species mass, respectively) (Figure 1). This factor showed a temporal variation, with remarkably high concentrations observed during the period of high relative humidity (RH) and low ozone concentration in the winter (Figure S6). The heterogeneous reactions on pre-existing particles in the polluted environment under high RH and low ozone conditions have been shown to play a key role in the formation of secondary aerosols compared to gas-phase photochemical processes (Sun et al., 2013; Niu et al., 2016; Ma et al., 2017b). Therefore, aqueous phase processes may be the major formation pathway for secondary inorganic aerosols in Beijing during the study period. Additionally, the factor showed a similar contribution (22-24%) to PM mass in winter at both sites. This value is lower than the value reported by Liu et al. (2019) at the other urban location (44%) in Beijing as a part of same APHH-Beijing campaign, although it should be noted that the sampling site and dates of sampling differed. We also noticed the source profile reported by Liu et al. (2019) contained a majority of all measured secondary inorganic species (>70%) as well as 20% of OC while the factor identified in the present study only accounted for ~55% of

secondary inorganic species and 11% of OC with remaining fractions identified in other factors. Thus, although the identification of the factor was “secondary” in both studies, they do not represent exactly the same source. The modelled difference in the contribution of this factor to PM mass may also be related to the uncertainties of the input species: a filter-based dataset was used in the present study while Liu et al., (2019) used online measurements.

The highest contribution to the PM mass was observed during the summertime, with an average concentration of  $11.1 \mu\text{g m}^{-3}$  (40%) and  $13.2 \mu\text{g m}^{-3}$  (48%) at IAP and PG, respectively (Figure 3).

**Traffic emissions.** The traffic emissions factor showed relatively high contributions to metallic elements, such as Zn (47%), Pb (57%), Mn (27%) and Fe (22%) (Figure 1). Zn is a major additive to lubricant oil. Zn and Fe can also originate from tyre abrasion, brake linings, lubricants and corrosion of vehicular parts and tailpipe emission (Pant and Harrison, 2012; Pant and Harrison, 2013; Grigoratos and Martini, 2015; Piscitello et al., 2021). As the use of Pb additives in gasoline has been banned since 1997 in Beijing, the observed Pb emissions may be associated with wear (tyre/brake) rather than fuel combustion (Smichowski et al., 2007). These results suggest the contribution of both exhaust and non-exhaust traffic emissions to this factor. Further insight on the type of non-exhaust emissions is hard to predict as these metal concentrations vary according to several parameters, such as traffic volume and patterns, vehicle fleet characteristics and the climate and geology of the region (Duong and Lee, 2011).

Traffic sources accounted for 9% and 6% of  $\text{PM}_{2.5}$  mass during the winter and summertime at IAP (Figure 3), corresponding to an average concentration of  $7.4 \mu\text{g m}^{-3}$  and  $1.8 \mu\text{g m}^{-3}$ , respectively. In addition, a low contribution (4%) was observed at PG during both seasons as PG experiences a low traffic volume. The contribution of the traffic source to the  $\text{PM}_{2.5}$  mass was found to be low compared to other studies conducted in the Beijing area; (14-20%) (Li et al., 2019; Tian et al., 2016; Yu et al., 2013; Liu et al., 2019), with the exception of a study by Ma et al. (2017a) where a similar contribution



413 was reported. The observed low contribution was further supported as a recent study also confirms  
414 that road traffic remains a dominant source of NO<sub>x</sub> and primary coarse PM, however, it only accounts  
415 a relatively small fraction of PM<sub>2.5</sub> mass at urban locations in Beijing (Harrison et al., 2021). It should  
416 be noted that nitrate that can be formed from NO<sub>x</sub> emitted from road traffic is not included in this  
417 factor. Despite the low factor contribution, the resolved chemical profile of this source was consistent  
418 with previously identified profiles linked to road traffic emissions in the Beijing area (Ma et al.,  
419 2017a; Yu et al., 2013). We noticed that OC/EC contribution in this factor is relatively low, while it  
420 may be higher in traffic emissions. However, given the modern gasoline fleet in Beijing (Jing et al.,  
421 2016), it is not unexpected to observe low OC and EC contribution. We do expect higher OC and EC  
422 contribution from diesel vehicles. In addition, there was no obvious seasonal variation as expected,  
423 though slightly higher concentrations were observed in the cold period, probably due to the typical  
424 atmospheric dynamics, and consequent poorer dispersion at this time of year.

425  
426 Metallic elements such as Mn, Fe and Zn were also used previously to indicate industrial activities  
427 (Li et al., 2017; Yu et al., 2013). Back trajectory analysis reveals the influence of local emissions with  
428 a slight regional transport during the winter period at both sites, dominated by north easterly flow  
429 (Figure S7). Therefore, there is a possibility that these elements could also come from the Hebei  
430 province where a large number of smelter industries are located. North-easterly and south-easterly  
431 flows were dominant during the summer period at IAP and PG with possible regional influence. These  
432 observations suggest that indeed this factor contains traffic aerosols, though a significant influence  
433 of industrial emissions cannot be ruled out.

434  
435 **Road dust.** This factor makes a major contribution to crustal species, such as Na<sup>+</sup>, Al and Fe (60%,  
436 48% and 34% of species in this factor respectively) suggesting this factor may represent the  
437 characteristics of a dust related source as reported previously (Kim and Koh, 2020). Such a high  
438 contribution of Na<sup>+</sup> in the identified factor was unexpected. Na is a major element of sea salt, sea-  
439 spray and marine aerosols (Viana et al., 2008), and has also been found to be enriched in fine

440 particulates from coal combustion (Takuwa et al., 2006). It is notable that a high proportion of Na<sup>+</sup>  
441 was attributed to road dust in a previous study conducted at the same urban site (Tian et al., 2016),  
442 and a crustal source seems likely, but has not been confirmed. In addition, the given factor also  
443 included significant contributions to Mn, Pb and Zn (26%, 23% and 20% of species in this factor  
444 respectively), which are associated with brake and tyre wear as mentioned above (Pant and Harrison,  
445 2012; Pant and Harrison, 2013; Grigoratos and Martini, 2015; Piscitello et al., 2021). High  
446 concentrations of Zn and Pb have also been reported for particles emitted from asphalt pavement  
447 (Canepari et al., 2008; Sörme et al., 2001). In addition, the ratio of Fe/Al observed in the factor  
448 chemical profile was 1.26, much higher than the value observed in the earth's crust (0.6), suggesting  
449 an anthropogenic origin of some Fe (Sun et al., 2005). This is likely as processes associated with  
450 vehicles, such as tyre/brake wear and road abrasion, can contaminate soil with metals, as the urban  
451 sampling site is located close to roads suggesting the resolved factor is likely linked to road dust  
452 emissions. These metals (Fe and Al) can also have industrial sources as already reported in the Beijing  
453 area (Wang et al., 2008; Tian et al., 2016; Yu et al., 2013; Li et al 2019). The Beijing-Tianjin-Hebei  
454 region is the largest urbanised megalopolis region in northern China, and home to many iron and steel  
455 making industries. Fe is characteristic components of iron and steel industry emissions (Li et al.,  
456 2019) while Al may also come from metal processing (Yu et al., 2013). However, disentangling the  
457 influence of industrial emissions would require further investigation.

458  
459 This source also made significant contributions to OC, EC and SO<sub>4</sub><sup>2-</sup> (11-19%) (Figure 1) and was  
460 consistent with the road dust source profiles observed previously in the Beijing area (Song et al.,  
461 2006; Song et al., 2007; Tian et al., 2016; Yu et al., 2013). This factor accounted for 20% of the PM<sub>2.5</sub>  
462 mass during the summertime (5.5 µg m<sup>-3</sup>) with exceptionally low contribution (3%) during the cold  
463 period at PG (Figure 3). However, the factor contribution at IAP was similar during both seasons. In  
464 addition, the contribution to PM mass at IAP in this study was similar to that reported by Tian et al.

465 (2016) and the studied urban site in both cases was the same. Crustal dust mass was also estimated  
466 based on the concentrations of Al, Si, Fe, Ca, and Ti using the equation below (Chan et al., 1997).

467 
$$\text{Crustal dust} = 1.16(1.9\text{Al} + 2.15\text{Si} + 1.41\text{Ca} + 1.67\text{Ti} + 2.09\text{Fe})$$

468  
469 A good correlation was observed between the estimated crustal dust and this factor during both  
470 seasons at PG (rural, winter:  $r^2 = 0.78$ ,  $m$  (slope) = 0.9; summer:  $r^2 = 0.94$ ,  $m=0.5$ ) and IAP (urban,  
471 winter:  $r^2 = 0.51$ ,  $m=1.3$ ; summer:  $r^2 = 0.68$ ,  $m=1.2$ ), highlighting that this may also contain a  
472 significant fraction of crustal dust (Figure S8). This suggests that the identified factor is not resolved  
473 cleanly and contains a mixed characteristic of road dust and crustal dust.

474  
475 **Soil dust.** This factor mainly represents wind-blown soils and was typically characterized by a high  
476 contribution to crustal elements, such as Ti (63%),  $\text{Ca}^{2+}$  (41%), Fe (27%) and Al (17%) (Figure 1).  
477 In addition, the contributions to Mn and Zn in the factor profile (Mn=24%, Zn=15%) suggest that the  
478 given source also included resuspended road dust but probably to a lesser extent. This source also  
479 showed a significant contribution to n-alkanes (e.g., C29, C31), derived from epicuticular waxes of  
480 higher plant biomass (Kolattukudy, 1976; Eglinton et al., 1962), with the highest contribution (37%)  
481 to C31. This suggests the presence of plant derived organic matter in the soil dust, which is also  
482 consistent with a high contribution to OC (15%).

483  
484 No clear seasonal variation was observed at PG. However, this factor showed a high contribution  
485 (35%,  $9.8 \mu\text{g m}^{-3}$ ) to  $\text{PM}_{2.5}$  mass during the summertime at IAP, while the contribution during other  
486 seasons at both sites was less than 10% (Figure 3). The factor profile resolved here was similar to the  
487 profile reported by Ma et al. (2017a) for soil dust, but their soil dust factor only showed a 10 %  
488 contribution to  $\text{PM}_{2.5}$  mass. In addition, other previous studies (Yu et al., 2013; Zhang et al., 2013)  
489 also reported significant contribution of soil dust to  $\text{PM}_{2.5}$  mass, suggesting that soil dust is an  
490 important contributor to  $\text{PM}_{2.5}$  mass in the Beijing area. It is also expected as Beijing is in a semi-arid

491 region and there are sparsely vegetated surfaces both within and outside the city. This factor also  
492 showed good agreement with the crustal fraction estimated from the element masses only during  
493 winter at PG ( $r^2=0.51$ ) and summer at IAP ( $r^2=0.58$ ). This again highlights the probable mixing of  
494 this source with other factors, or mis-attribution. Back trajectory analysis also indicates the influence  
495 of regional transport during the summer period at IAP, dominated by south easterly-westerly flow  
496 (Figure S9) due to high windspeeds ( $3.6 \text{ m s}^{-1}$ ). Therefore, there is a possibility that the high  
497 contribution is linked to long-range transport in advected air masses. A recent study (Gu et al., 2020)  
498 conducted in Beijing showed the high concentrations of more oxidised aerosols during summer due  
499 to enhanced photochemical processes; however, such type of source was not resolved due to a lack  
500 of filter based markers. This suggests the given source may contain some influence from an  
501 unidentified/unresolved SOC fraction. Although the most plausible attribution appears to be to soil  
502 dust, it is not fully resolved from other sources.

503  
504 The use of Si in PMF could provide a better understanding on these dust related sources. However, it  
505 is not used in the present PMF input due to high number of missing data points. The sensitivity of  
506 PMF results to the use of Si has also been investigated by adding Si to the input matrix and providing  
507 high uncertainty to the missing data. No change was observed in the factor profile and temporal  
508 variation of the resolved factors compared to the present one. In addition, we also noticed a good  
509 correlation between Si and Al, where Al has been used in PMF (Figure S10). Several PMF runs were  
510 also made with inorganic data only, however the resolved factors were either mixed or hard to  
511 identify. In addition, attempts to improve the PMF results by varying the input species and by  
512 analysing data for the IAP and PG sites separately did not offer any advantage.

513

514

515

## 3.2 Comparison of Filter-Based PMF Results with other Receptor Modelling Approaches on the same Dataset

The source apportionment results from PMF were compared with those from CMB on the same filter-based composition data and PMF performed on other measurements (i.e. online AMS ( $\text{PM}_{10}$ ), offline AMS ( $\text{PM}_{2.5}$ )) to get a deeper insight into the identified PMF factors and their origins (Figures 4, 5, 6 and 7). The CMB method resulted in the estimation of eight OC sources (i.e., vegetative detritus, residential coal combustion (CC), industrial CC, cooking, diesel vehicles, gasoline vehicles, biomass burning, other OC), including one secondary factor (Other OC) at both sites (IAP and PG). The online AMS datasets allowed the identification of 6 OA (MOOOA (more oxidised oxygenated OA), LOOOA (low more oxidised oxygenated OA), OPOA (oxidised primary OA), BBOA (biomass burning OA), COA (cooking OA), CCOA (coal combustion OA) factors during winter at IAP, while analyses on the offline AMS measurements resolved 4 OA (OOA, BBOA, COA, CCOA) factors.

For these analyses, OC concentrations related to the online/offline AMS OA factors were further calculated by applying OC-to-OA conversion factors specific to each source, i.e., 1.35 for coal combustion organic carbon (Sun et al., 2016), 1.38 for cooking organic carbon, 1.58 for biomass burning organic carbon (Xu et al., 2019), and 1.78 for the oxygenated fraction (Huang et al., 2010) and used to evaluate the OC concentrations of relevant OA factors.

Only OC equivalent concentrations were used to perform comparison for all approaches. OC mass closure was also verified at IAP during the wintertime by investigating the relation between: OC modelled by online AMS PMF vs filter based PMF ( $r^2=0.7$ , slope=1.17), OC measured vs OC modelled by filter based PMF ( $r^2=0.7$ , slope=1.07), OC measured vs OC modelled by online AMS PMF ( $r^2=0.9$ , slope=0.92), OC modelled by offline AMS PMF vs OC model by filter based PMF ( $r^2=0.6$ , slope=0.75), OC measured vs OC modelled by offline AMS PMF ( $r^2=0.9$ , slope=1.41), and OC measured vs WSOA (offline AMS) ( $r^2=0.9$ , slope=0.85) (Figure S11). The comparison of OC

542 modelled by PMF and CMB was also investigated at IAP ( $r^2=0.8$ , slope=1.05) and PG ( $r^2=0.6$ ,  
 543 slope=1.78) (Figure S12). All source apportionment approaches showed a fairly good agreement in  
 544 reconstructing the total OC mass, justifying their direct comparison. In addition, it should be noted  
 545 that the difference in the sampling size cut-off between online AMS (NR-PM<sub>1</sub>) and filter  
 546 measurements (PM<sub>2.5</sub>) may contribute to the differences observed in the source apportionment  
 547 results. Therefore, we also compared the relation between NR-PM measured vs PM measured  
 548 ( $r^2=0.96$ , slope=0.92), and NR-PM measured vs PM modelled by filter based PMF ( $r^2=0.9$ ,  
 549 slope=1.29) (Figure S13). The agreements observed suggest that the most of the PM<sub>2.5</sub> mass was  
 550 accounted for by the PM<sub>1</sub> fraction, indicating that the difference in the size-cut off is relatively small.

551

#### 552 (a) With CMB results at IAP

553 Resolved CMB and PMF factors were compared including data from both seasons at IAP and PG  
 554 (Figure 4). A good correlation ( $r^2=0.6$ ,  $n=68$ ,  $p<0.05$ ) was observed between biomass burning factors,  
 555 suggesting that this source was well resolved using both approaches (Figure 4). However, a slightly  
 556 higher concentration was reported by the CMB model (2.0 and 1.6  $\mu\text{g m}^{-3}$  by CMB and PMF  
 557 respectively). Individual coal combustion factors (industrial/residential) did not show any  
 558 significant correlation ( $r^2<0.2$ ) with the coal combustion factor identified using PMF, although the  
 559 total coal combustion fraction from CMB, the sum of industrial and residential fractions, did show  
 560 an improved correlation ( $r^2=0.4$ ). Some improvement on the correlation was seen if two outlier  
 561 datapoints were removed (see Figure 4). A likely reason is that PMF did not resolve coal combustion  
 562 and biomass burning factors well as both factors presented a strong seasonal pattern with high  
 563 concentrations during the winter. Another possibility is the difficulty in resolving primary and  
 564 secondary fractions due to a lack of secondary organic markers used in the study. This was further  
 565 supported by the fact noted above that the PMF biomass burning factor also contained some signal  
 566 from coal combustion activities. The sum of coal combustion and biomass burning factors from both

approaches showed a good correlation ( $r^2=0.7$ ,  $n=68$ ,  $p<0.05$ ), suggesting a common emission pattern (e.g., high in winter and low in summer), making it challenging to resolve them. Factors linked to vehicle emissions did not show any correlation. A weak correlation ( $r^2=0.3$ ,  $n=68$ ,  $p<0.05$ ) was observed between Other OC from CMB, a proxy for the secondary organic fraction and the PMF secondary inorganics factor. In addition, other OC also weakly correlated with soil dust ( $r^2=0.22$ ,  $n=34$ ,  $p<0.05$ ) in summer, suggesting the mixing of unresolved secondary fraction with soil dust profile and supports the hypothesis discussed above. It should be noted that other OC could also contain unresolved primary fractions as PMF results indicated substantial influence of industrial emissions and dust related sources. However, the source profiles related to industrial emissions and dust were not accounted for in the CMB model (Xu et al., 2021).

577

#### 578 (b) With CMB results at PG

The comparison was also made using data from both seasons at PG (Figure 5). Biomass burning aerosols showed a good correlation for both approaches ( $r^2=0.7$ ,  $n=20$ ,  $p<0.05$ ) but a substantially higher concentration was estimated by the CMB model ( $5.1 \mu\text{g m}^{-3}$  and  $2.0 \mu\text{g m}^{-3}$  by CMB and PMF respectively). A significant correlation was also seen between traffic related factors from CMB and PMF (gasoline-CMB vs traffic ( $r^2=0.6$ ,  $n=20$ ,  $p<0.05$ ), diesel-CMB vs traffic ( $r^2=0.6$ ,  $n=20$ ,  $p<0.05$ )), indicating that traffic sources resolved using PMF at the PG site may have included signals from both diesel and gasoline vehicles; however it was not conclusive at the IAP site, as discussed above. This suggests the traffic source resolved using PMF may contain particles linked to traffic emissions, but the influence of other sources is prominent at IAP and resulted in poor correlation. In addition, for traffic related factors from CMB, both showed a higher concentration (gasoline-CMB= $0.8 \mu\text{g m}^{-3}$ , diesel-CMB= $4.5 \mu\text{g m}^{-3}$ , traffic-PMF= $0.2 \mu\text{g m}^{-3}$ ). As with IAP, no significant correlation was observed between coal combustion factors from both approaches. The sum of coal combustion and biomass burning factors from both approaches also did not present a good correlation ( $r^2=0.3$ ,  $n=20$ ,

p<0.05). This highlights the limitation of these methodologies to apportion sources when extreme meteorological conditions may lead to high internal mixing of sources. Unfavourable dispersion conditions have been previously observed in the Beijing region during severe haze events in winter (Wang et al., 2014). A high correlation was observed between Other OC (CMB) and secondary inorganics (PMF) ( $r^2=0.7$ ,  $n=20$ ,  $p<0.05$ ). In addition, Other OC also showed a very high correlation with the biomass burning factor resolved from PMF ( $r^2=0.9$ ,  $n=20$ ,  $p<0.05$ ). This suggests that the biomass burning factor in PMF may contain a substantial amount of aged aerosols since carbon emitted during biomass burning is in some cases oxygenated and water soluble (Lee et al., 2008b) and is subject to rapid oxidation in the atmosphere.

#### (c) With online AMS PMF factors at IAP (winter)

BBOC (biomass burning OC) from PMF-AMS analysis agreed well with that from PMF ( $r^2=0.7$ ,  $n=27$ ,  $p<0.05$ ;  $4.0 \mu\text{g m}^{-3}$  and  $3.1 \mu\text{g m}^{-3}$  by online AMS and PMF, respectively) (Figure 6). Coal combustion related factors showed a modest correlation (CCOC (coal combustion OC) vs coal combustion-PMF,  $r^2=0.4$ ,  $n=27$ ,  $p<0.05$ ) but the mass concentration of the coal combustion source by PMF ( $11.3 \mu\text{g m}^{-3}$ ) is significantly higher than by PMF-AMS (CCOC= $4.7 \mu\text{g m}^{-3}$ ). This may partly be due to the different size cut offs used by these measurements ( $\text{PM}_{10}$  for AMS vs  $\text{PM}_{2.5}$ ). In addition, significant improvement on the correlation was seen if two outlying points were removed ( $r^2=0.8$ , see Figure 6). Oxygenated fractions from AMS, MOOOC (more oxidised oxygenated OC) and LOOOC (low oxidised oxygenated OC) also exhibited a good correlation with secondary inorganics (LOOOC vs secondary inorganics ( $r^2=0.6$ ,  $n=27$ ,  $p<0.05$ , LOOOC= $2.9 \mu\text{g m}^{-3}$ , secondary inorganics= $1.6 \mu\text{g m}^{-3}$ ), MOOOC vs secondary inorganics ( $r^2=0.7$ ,  $n=27$ ,  $p<0.05$ , MOOOC= $4.4 \mu\text{g m}^{-3}$ )). This was also confirmed by LOOOC and MOOOC showing a good correlation with  $\text{NO}_3^-$  and  $\text{SO}_4^{2-}$  previously (Cao et al., 2017). The formation of both secondary inorganic aerosol and oxygenated organic aerosol is dependent upon largely the same set of oxidant species, notably but not solely the hydroxyl and nitrate radicals. In both cases there are also both homogeneous and



heterogeneous (aqueous phase) pathways, so conditions which promote the formation of oxidised organic aerosol will also favour formation of secondary inorganic aerosol, and hence a correlation is to be expected, and is often observed (Hu et al., 2016; Zhang et al., 2011). In addition, both oxygenated fractions were also found to be correlated with biomass burning aerosols (LOOOC vs biomass burning-PMF ( $r^2=0.7$ ,  $n=27$ ,  $p<0.05$ ), MOOOC vs biomass burning-PMF ( $r^2=0.6$ ,  $n=27$ ,  $p<0.05$ )). This further highlights a potentially important role of biomass burning activity in SOA formation at IAP. A good correlation was also observed between OPOC (oxidised primary OC) and secondary inorganics and biomass burning ( $r^2=0.7$ ,  $n=27$ ,  $p<0.05$ ).

626

#### 627 (d) Offline AMS PMF factors at IAP (winter)

BBOC from PMF-offline AMS analysis showed a good correlation with that from PMF ( $r^2=0.6$ ,  $n=32$ ,  $p<0.05$ ) (Figure 7) but the mass concentration of BBOC ( $4.6 \mu\text{g m}^{-3}$ ) is higher than biomass burning ( $3.1 \mu\text{g m}^{-3}$ ) from PMF. This was also noticed above while comparing with BBOC resolved using online AMS PMF, suggesting a potential uncertainty in estimating the source contribution from biomass burning. The uncertainty in filter-based PMF analysis could be related to model error. This was further supported as biomass burning factor also made significant contributions to  $\text{Ca}^{2+}$  (15%), Ni (30%), Cu (50%), and Al (35%), and these species are not necessarily from biomass burning emissions but they were not resolved by PMF. In addition, the uncertainties linked to PMF-AMS analysis could also contribute. A high correlation was noticed for secondary factors resolved using both approaches (OOC (oxygenated OC) vs Secondary inorganics,  $r^2=0.8$ ,  $n=32$ ,  $p<0.05$ ). OOC also showed a good correlation with the biomass burning factor (OOC vs biomass burning-PMF,  $r^2=0.7$ ,  $n=32$ ,  $p<0.05$ ). This supports the hypothesis discussed previously on the origin of oxygenated fractions.

641

Overall, the comparison of filter based PMF results was in broad agreement with other receptor modelling approaches applied on the same dataset. However, large discrepancies were also observed

644 for some factors / sources. Common sources such as biomass burning and coal combustion were well  
645 resolved using all approaches with some exceptions observed when using filter based PMF approach.  
646 This could be linked to internal mixing of sources when the influence of climate and local  
647 meteorology on both sources is predominant and making it challenging to resolve using PMF. A good  
648 agreement was also observed between secondary inorganic aerosols and secondary fractions resolved  
649 using other approaches. However, sources identified based on metal signatures using PMF indicated  
650 some mixing or mis-attribution. For example, the influence of unresolved SOC on the soil dust profile  
651 was observed during summer.

652

### 653 **3.3. Comparison with Previous PMF Source Apportionment Results in Beijing**

654 In this section an attempt has been made to understand the PM sources identified in the Beijing  
655 metropolitan area by previous studies. The goal was here to assess the previous PMF source  
656 apportionment results and report any discrepancies noticed in the resolved sources using PMF. This  
657 may provide useful insight on sources resolved in the present study and also in exploring the issues  
658 associated with filter based PMF modelling in the Beijing metropolitan area. Details of the studies  
659 conducted to evaluate PM sources using a PMF model applied to inorganic and organic markers in  
660 the Beijing metropolitan area are presented in Table S5 and the major outcomes are discussed  
661 hereafter.

662

663 Overall, these previous PMF studies provide insights on PM sources in the Beijing metropolitan area  
664 (Li et al., 2019; Ma et al., 2017a; Tian et al., 2016; Yu et al., 2013; Song et al., 2007; Song et al.,  
665 2006; Liu et al., 2019; Wang et al., 2008; Zhang et al., 2013). The major identified sources are dust,  
666 traffic emissions, coal combustion, industrial activity, secondary inorganic aerosols and biomass  
667 burning. Although there is a general issue of their inability to identify sources such as secondary  
668 organic aerosol and cooking emissions, similar to the present study, due to the lack of organic markers  
669 used in the PMF model to apportion these sources. However, beyond this, their PMF outcomes were

not consistent. Large discrepancies between the sources were seen (Table S5) based on the sources identified as well as their contribution to PM mass concentrations. Several factors could cause these differences such as the chemical species used as input in the PMF model, the period of the study, identification of sources based on chemical signatures and changes to the sources with time.

Input species considered within the previous studies were combinations of water-soluble ions, metallic elements, OC and EC. Similar input species were used in all of these studies, with the exception of the studies by Yu et al. (2013) and Li et al. (2019) who used only metallic elements for the source apportionment. As shown in this study, including organic markers may help to resolve some of the primary sources.

Another important parameter, the chemical species used for identifying sources were not always consistent. For example, coal combustion was resolved based on high contribution of OC, EC, and Cl present in the factor profile by Zhang et al. (2013), Wang et al. (2008), Song et al. (2007) and Song et al. (2006), in accordance with source profiles determined in the laboratory (Zheng et al., 2005). High Cl associated with fine aerosols in winter is a distinctive feature in Beijing and even around inland China, which is ascribed to coal combustion (Wang et al., 2008). Contrarily, Tian et al. (2016) identified coal combustion based on a high contribution of OC and EC, while the high contribution of Cl was attributed to a biomass burning source, similar to another study (Ma et al., 2017a). In other studies (Li et al., 2019; Yu et al., 2013; Liu et al., 2019) coal combustion was resolved based on the presence of metallic elements such as V, Se, Co, Cd, As and Ni, where V and Ni are widely used markers for oil combustion (Mazzei et al., 2008). High loadings of As and Se have also been reported as a typical source characteristic of coal combustion (Vejahati et al., 2010). Similar to coal combustion, biomass burning was often characterised using the presence of K (Li et al., 2019; Tian et al., 2016; Yu et al., 2013; Song et al., 2007; Song et al., 2006; Zhang et al., 2013; Liu et al., 2019; Wang et al., 2008), a typical marker of biomass burning. Farming in Beijing's suburban districts has

696 been extensive in recent years. Burning of the crop remnants and fallen leaves by farmers in autumn  
697 and winter results in the enhanced emissions of K. In addition, the contributions of Cl and Na were  
698 also considered for the identification of these sources in some cases, depending on the species used  
699 within the input (Song et al., 2007; Song et al., 2006; Tian et al., 2016). This highlights the fact that  
700 none of the studies have used organic markers such as picene and levoglucosan which are very  
701 specific to these combustion sources as discussed before, which may cause uncertainty in the resolved  
702 sources. However, in the present study the use of organic markers played a key role in the  
703 identification of these sources and their better apportionment. Despite this, some issues were observed  
704 with these identified sources during winter due to extreme meteorological conditions as well as co-  
705 emission of these aerosols at the same time, probably indicative of poor performance of the PMF  
706 model under certain conditions.

707

708 Other important sources linked to traffic emissions, industrial activities and dust, are commonly  
709 resolved among all the studies. The characterisation of these sources was predominantly based on the  
710 metallic elements. For example, Zn, Cu, and Pb including sometimes EC were most often used to  
711 characterise traffic emissions among all previous studies. Both Zn and Cu have been identified within  
712 brake linings and tyre fragments (Thorpe and Harrison, 2008) and Pb has been used in the past within  
713 gasoline as an anti-knock additive in China (Li et al., 2019). However, Cu and Zn can also serve as  
714 indicators for industrial sources (Li et al., 2017; Yu et al., 2013). Other metallic elements (e.g., Sb,  
715 Cr, Mn, K, Br and Ba) were also considered in certain cases to trace traffic emissions (Ma et al.,  
716 2017a; Tian et al., 2016; Yu et al., 2013). However, a high contribution of Cr, Mn and sometimes Fe  
717 to the given sources has also been attributed to industrial activities. Both Cr and Cr-containing  
718 compounds are widely used in metallurgy, electroplating, pigment, leather and other industries  
719 (Dall'Osto et al., 2013). A previous study found that ferrous metallurgy could emit Mn (Querol et al.,  
720 2006). Furthermore, both Fe and Mn are characteristic components of iron and steel industry  
721 emissions. In addition, Co, Mg, Al, Ca, Cd, Pb, Tl, Zn, V, Ni and Cu were also considered for the

722 apportionment of industrial sources (Tian et al., 2016; Yu et al., 2013). Zhang et al. (2013) identified  
723 a mixed source of traffic and incineration emissions, based on high loading of Cu, Zn, Cd, Pb, Sb,  
724 Sn, Mo,  $\text{NO}_3^-$  and EC. In the present study, the assignment of road traffic emissions was based on  
725 high loadings of Zn and Pb. It was also seen that the given source may contain some influence from  
726 industrial activities, as the industrial contribution was not resolved like previous studies and probably  
727 accounted in other factors. Thus, it is clear that these metals could belong to several sources and their  
728 proper assignment to respective sources is difficult in the complex environment.

729

730 The same issue was observed with the assignments of dust type (dust/road dust/soil dust/mineral  
731 dust/yellow dust/local dust) sources. Although the dust type sources were often found to be composed  
732 of crustal elements (e.g., Ca, Mg, Si, Ti, Al, Fe), the attribution of crustal elements to a particular  
733 source was not consistent from one study to another previously. The two dust sources (road dust and  
734 soil dust) identified in the present study also indicated mixing with other factors.

735

736 The identification of the secondary inorganic aerosol factors was often based on the high contribution  
737 of water soluble ions ( $\text{NO}_3^-$ ,  $\text{SO}_4^{2-}$ ,  $\text{NH}_4^+$ ), consistent with other studies (Ma et al., 2017a; Song et al.,  
738 2007; Song et al., 2006; Tian et al., 2016; Liu et al., 2019; Wang et al., 2008; Zhang et al., 2013).  
739 These results highlight the role of chemical species used in characterising source profiles and their  
740 influence on the variability noticed in the Beijing metropolitan area. This issue arises because many  
741 of these species are not source specific, making it challenging to directly link PMF factors to sources.  
742 Pant and Harrison (2012), reviewing receptor modelling studies from India, noted a tendency to  
743 attribute metal-rich source profiles to “industry” in a rather casual manner without evidence of local  
744 industrial sources.

745

746 The change in sources and emissions over the course of time due to stringent emissions regulations  
747 could also be considered plausible for the observed variability in the chemical profile and contribution

748 of identified sources. Li et al. (2019) showed levels of trace metals (V, Cr, Mn, As, Cd and Pb)  
749 decreased more than 40% due to the emission regulations, while crustal elements decreased  
750 considerably (4–45%), suggesting emissions from anthropogenic activities were suppressed. A  
751 reduction in the contribution of sources such as dust and industrial activity was observed in the present  
752 study and another recent study performed by Liu et al. (2019) relative to the previous ones, indicating  
753 the effect of regulatory measures on the contribution of identified sources to PM<sub>2.5</sub>. However, the  
754 concentration of the majority of metallic elements (K, Cr, Mn, Fe, Co, Cu, Zn, As, Ag, Cd and Pb)  
755 increased when pollution levels changed from clean days to heavily polluted days. This highlights  
756 that specific atmospheric conditions could also play a major role for the observed variability. Another  
757 factor is the time of year when these studies were conducted as some of the identified sources (e.g.,  
758 coal combustion and biomass burning) exhibit typical seasonal patterns. During a low concentration  
759 period, PMF models may have difficulty in resolving sources, leading to mixing of factors.

760  
761 Overall, the present study provides a view of existing PM<sub>2.5</sub> sources in the Beijing metropolitan area  
762 by applying the PMF model to a filter-based dataset, which included water soluble ions, metals and  
763 organic markers. Despite this, factors that were resolved based on metal signatures were not fully  
764 resolved and indicate a mixing of different sources. As a part of same campaign, also discussed above,  
765 Liu et al. (2019) used a similar approach by applying PMF on high resolution (1-hour) data, which  
766 included OC, EC, ions, and metals, and did not encounter any issue. However, previous filter based  
767 PMF studies conducted in the Beijing region that mostly included ions and metals in their input  
768 dataset often showed difficulty in the proper assignment of metals to their respective sources. Even  
769 the use of metal signatures from one to another study was not consistent. This highlights that the low  
770 temporal resolution of filter data could not capture fast occurring atmospheric processes in Beijing,  
771 and may lead to a “blurring” of sources by the long averaging period. Atmospheric circulation and  
772 dynamic mechanisms play a key role in persistent haze events in Beijing during the cold period (Wu  
773 et al., 2017; Feng et al., 2014). Such events are associated with the high pollution periods and will

offer opportunities for chemical and physical transformation within the aerosol that lead to contravention of the requirement of receptor models for preservation of chemical profiles between source and receptor.

777

#### 778 **4. CONCLUSION**

This study presents the outcomes of PMF performed on the combined dataset collected at two sites (IAP and PG) in the Beijing metropolitan area, including their comparison with source apportionment results from other approaches or based on different measurements. The PMF analysis resulted in the identification of seven sources: coal combustion, biomass burning, oil combustion, secondary inorganics, traffic emissions, road dust and soil dust. These results were in a good agreement with previously published source apportionment results made using PMF. However, factors that were resolved based on metal signatures were not fully resolved and indicate an internal mixing of different sources. In particular, soil dust, road dust and some industrial sources have many elements in common and are very difficult to distinguish.

788

PMF results were compared with sources resolved from CMB and with PMF performed on other measurements (online AMS, offline AMS). Results showed a broad agreement with some notable exceptions. While this study provides some confirmatory evidence on PM<sub>2.5</sub> source apportionment in Beijing, it highlights weaknesses of the PMF method when applied in this locality, and the results should be viewed in the context of studies using other methods such as CMB which appear able to give a more comprehensive view of the key sources affecting air quality. No industrial source profiles were used as inputs to the CMB model reported here, so CMB offers no further insights into possible contributions from industry.

797

#### 798 **AUTHOR CONTRIBUTIONS**

799 This study was conceived by ZS and RMH. DS performed the PMF analysis and wrote the paper with  
800 the help of Z.S. and R.M.H. T.V.V. and D.L. conducted the aerosol sampling and laboratory-based  
801 chemical analyses. X.W. and J.X. conducted the CMB modelling at PG and IAP sites, respectively.  
802 All authors discussed the paper and approved the final version for publication.

803  
804 **COMPETING INTERESTS**

805 The authors declare that they have no conflict of interest.

806  
807 **SPECIAL ISSUE STATEMENT**

808 This article is part of the special issue “In-depth study of air pollution sources and processes within  
809 Beijing and its surrounding region (APHH-Beijing) (ACP/AMT inter-journal SI)”. It is not associated  
810 with a conference.

811  
812 **FINANCIAL SUPPORT**

813 This research has been supported by the Natural Environment Research Council (APHH and SOA  
814 grants): NE/N007190/1 (AIRPOLL-Beijing), NE/S006699/1 (SOA).

815



## 816 REFERENCES

- 817 Amato, F., Pandolfi, M., Escrig, A., Querol, X., Alastuey, A., Pey, J., Perez, N., and Hopke, P. K.:  
 818 Quantifying road dust resuspension in urban environment by Multilinear Engine: A comparison with  
 819 PMF2, *Atmos. Environ.*, 43, 2770-2780, <https://doi.org/10.1016/j.atmosenv.2009.02.039>, 2009.
- 820  
 821 Amato, F., and Hopke, P. K.: Source apportionment of the ambient PM<sub>2.5</sub> across St. Louis using  
 822 constrained positive matrix factorization, *Atmos. Environ.*, 46, 329-337,  
 823 <https://doi.org/10.1016/j.atmosenv.2011.09.062>, 2012.
- 824  
 825 Batterman, S., Xu, L., Chen, F., Chen, F., and Zhong, X.: Characteristics of PM<sub>(2.5)</sub> Concentrations  
 826 across Beijing during 2013-2015, *Atmos. Environ.* (Oxford, England: 1994), 145, 104-114,  
 827 [10.1016/j.atmosenv.2016.08.060](https://doi.org/10.1016/j.atmosenv.2016.08.060), 2016.
- 828  
 829 Bi, X., Simoneit, B. R. T., Sheng, G., and Fu, J.: Characterization of molecular markers in smoke  
 830 from residential coal combustion in China, *Fuel*, 87, 112-119,  
 831 <https://doi.org/10.1016/j.fuel.2007.03.047>, 2008.
- 832  
 833 Boucher, O., Randall, D., Artaxo, P., Bretherton, C., Feingold, G., Forster, P., Kerminen, V.-M.,  
 834 Kondo, Y., Liao, H., and Lohmann, U.: Clouds and aerosols, in: *Climate change 2013: the physical  
 835 science basis. Contribution of Working Group I to the Fifth Assessment Report of the  
 836 Intergovernmental Panel on Climate Change*, Cambridge University Press, 571-657, 2013.
- 837  
 838 Cai, T., Zhang, Y., Fang, D., Shang, J., Zhang, Y., and Zhang, Y.: Chinese vehicle emissions  
 839 characteristic testing with small sample size: Results and comparison, *Atmospheric Pollution  
 840 Research*, 8, 154-163, <https://doi.org/10.1016/j.apr.2016.08.007>, 2017.
- 841  
 842 Canepari, S., Perrino, C., Olivieri, F., and Astolfi, M. L.: Characterisation of the traffic sources of  
 843 PM through size-segregated sampling, sequential leaching and ICP analysis, *Atmos. Environ.*, 42,  
 844 8161-8175, <https://doi.org/10.1016/j.atmosenv.2008.07.052>, 2008.
- 845  
 846 Cao, L., Zhu, Q., Huang, X., Deng, J., Chen, J., Hong, Y., Xu, L., and He, L.: Chemical  
 847 characterization and source apportionment of atmospheric submicron particles on the western coast  
 848 of Taiwan Strait, China, *J. Environ. Sci.*, 52, 293-304, <https://doi.org/10.1016/j.jes.2016.09.018>,  
 849 2017.
- 850  
 851 Chan, Y., Simpson, R., McTainsh, G., Vowles, P., Cohen, D., and Bailey, G. J. A. E.: Characterisation  
 852 of chemical species in PM<sub>2.5</sub> and PM<sub>10</sub> aerosols in Brisbane, Australia, *Atmos. Environ.*, 31, 3773-  
 853 3785, 1997.
- 854  
 855 Dall'Osto, M., Querol, X., Amato, F., Karanasiou, A., Lucarelli, F., Nava, S., Calzolari, G., and Chiari,  
 856 M.: Hourly elemental concentrations in PM<sub>2.5</sub> aerosols sampled simultaneously at urban background  
 857 and road site during SAPUSS - diurnal variations and PMF receptor modelling, *Atmos. Chem. Phys.*,  
 858 13, 4375, 2013.
- 859  
 860 Draxler, R.: *Hysplit4 User's Guide*. NOAA Tech. Memo. ERL ARL-230, 35 pp.  
 861 [http://www.arl.noaa.gov/documents/reports/hysplit\\_user\\_guide.pdf](http://www.arl.noaa.gov/documents/reports/hysplit_user_guide.pdf), 1999.
- 862  
 863 Duong, T. T. T., and Lee, B.-K.: Determining contamination level of heavy metals in road dust from  
 864 busy traffic areas with different characteristics, *J. Environ. Manage.*, 92, 554-562,  
 865 <https://doi.org/10.1016/j.jenvman.2010.09.010>, 2011.
- 866

- Duvall, R. M., Majestic, B. J., Shafer, M. M., Chuang, P. Y., Simoneit, B. R. T., and Schauer, J. J.: The water-soluble fraction of carbon, sulfur, and crustal elements in Asian aerosols and Asian soils, *Atmos. Environ.*, 42, 5872-5884, <https://doi.org/10.1016/j.atmosenv.2008.03.028>, 2008.
- Eglinton, G., Gonzalez, A. G., Hamilton, R. J., and Raphael, R. A.: Hydrocarbon constituents of the wax coatings of plant leaves: A taxonomic survey, *Phytochemistry*, 1, 89-102, [https://doi.org/10.1016/S0031-9422\(00\)88006-1](https://doi.org/10.1016/S0031-9422(00)88006-1), 1962.
- Feng, X., Li, Q., Zhu, Y., Wang, J., Liang, H., and Xu, R.: Formation and dominant factors of haze pollution over Beijing and its peripheral areas in winter, *Atmos. Pollut. Res.*, 5, 528-538, <https://doi.org/10.5094/APR.2014.062>, 2014.
- GBD MAPS Working Group: Burden of Disease Attributable to Coal-Burning and Other Major Sources of Air Pollution in China, Special Report 20, Health Effects Institute, Boston, MA, 2016.
- Grigoratos, T., and Martini, G.: Brake wear particle emissions: a review, *Environ. Sci. Pollut. Res.*, 22, 2491-2504, 10.1007/s11356-014-3696-8, 2015.
- Gu, Y., Huang, R.-J., Li, Y., Duan, J., Chen, Q., Hu, W., Zheng, Y., Lin, C., Ni, H., Dai, W., Cao, J., Liu, Q., Chen, Y., Chen, C., Ovadnevaite, J., Ceburnis, D., and O'Dowd, C.: Chemical nature and sources of fine particles in urban Beijing: Seasonality and formation mechanisms, *Environ. Intl.*, 140, 105732, <https://doi.org/10.1016/j.envint.2020.105732>, 2020.
- Guo, H., Zhou, J., Wang, L., Zhou, Y., Yuan, J., and Zhao, R.: Seasonal variations and sources of carboxylic acids in PM<sub>2.5</sub> in Wuhan, China, *Aerosol Air. Qual. Res.*, 15, 517-528, 10.4209/aaqr.2014.02.0040, 2015.
- Harrison, R. M., Vu, T. V., Jafar, H., and Shi, Z.: More mileage in reducing urban air pollution from road traffic, *Environ. Int.*, 149, 106329, <https://doi.org/10.1016/j.envint.2020.106329>, 2021.
- He, G., Pan, Y., and Tanaka, T.: The short-term impacts of COVID-19 lockdown on urban air pollution in China, *Nature Sustainability*, 3, 1005-1011, 10.1038/s41893-020-0581-y, 2020.
- Heal, M. R., Kumar, P., and Harrison, R. M.: Particles, air quality, policy and health, *Chem. Soc. Rev.*, 41, 6606-6630, 2012.
- Henry, R., Norris, G. A., Vedantham, R., and Turner, J. R.: Source Region Identification Using Kernel Smoothing, *Environ. Sci. Technol.*, 43, 4090-4097, 10.1021/es8011723, 2009.
- Herrera Murillo, J., Campos Ramos, A., Ángeles García, F., Blanco Jiménez, S., Cárdenas, B., and Mizohata, A.: Chemical composition of PM<sub>2.5</sub> particles in Salamanca, Guanajuato Mexico: Source apportionment with receptor models, *Atmos. Res.*, 107, 31-41, 10.1016/j.atmosres.2011.12.010, 2012.
- Hopke, P. K.: Review of receptor modeling methods for source apportionment, *JAWMA*, 66, 237-259, 10.1080/10962247.2016.1140693, 2016.
- Hu, W., Hu, M., Hu, W., Jimenez, J. L., Yuan, B., Chen, W., Wang, M., Wu, Y., Chen, C., Wang, Z., Peng, J., Zeng, L., and Shao, M.: Chemical composition, sources, and aging process of submicron aerosols in Beijing: Contrast between summer and winter, 121, 1955-1977, 10.1002/2015jd024020, 2016.

919 Huang, X., Tang, G., Zhang, J., Liu, B., Liu, C., Zhang, J., Cong, L., Cheng, M., Yan, G., Gao, W.,  
 920 Wang, Y., and Wang, Y.: Characteristics of PM<sub>2.5</sub> pollution in Beijing after the improvement of air  
 921 quality, *J. Environ. Sci.*, 100, 1-10, <https://doi.org/10.1016/j.jes.2020.06.004>, 2021.  
 922  
 923 Huang, X. F., He, L. Y., Hu, M., Canagaratna, M. R., Sun, Y., Zhang, Q., Zhu, T., Xue, L., Zeng, L.  
 924 W., Liu, X. G., Zhang, Y. H., Jayne, J. T., Ng, N. L., and Worsnop, D. R.: Highly time-resolved  
 925 chemical characterization of atmospheric submicron particles during 2008 Beijing Olympic Games  
 926 using an Aerodyne High-Resolution Aerosol Mass Spectrometer, *Atmos. Chem. Phys.*, 10, 8933-  
 927 8945, 10.5194/acp-10-8933-2010, 2010.  
 928  
 929  
 930 Jaeckels, J. M., Bae, M.-S., and Schauer, J. J.: Positive matrix factorization (PMF) analysis of  
 931 molecular marker measurements to quantify the sources of organic aerosols, *Environ. Sci. Technol.*,  
 932 41, 5763-5769, 2007.  
 933  
 934 Ji, D., Li, L., Wang, Y., Zhang, J., Cheng, M., Sun, Y., Liu, Z., Wang, L., Tang, G., and Hu, B. J. A.  
 935 E.: The heaviest particulate air-pollution episodes occurred in northern China in January, 2013:  
 936 Insights gained from observation, *Atmos. Environ.*, 92, 546-556,  
 937 doi.org/10.1016/j.atmosenv.2014.04.048, 2014.  
 938  
 939 Jing, B., Wu, L., Mao, H., Gong, S., He, J., Zou, C., Song, G., Li, X., and Wu, Z.: Development of a  
 940 vehicle emission inventory with high temporal-spatial resolution based on NRT traffic data and its  
 941 impact on air pollution in Beijing – Part 1: Development and evaluation of vehicle emission  
 942 inventory, *Atmos. Chem. Phys.*, 16, 3161-3170, 10.5194/acp-16-3161-2016, 2016.  
 943  
 944 Kim, E.-A., and Koh, B.: Utilization of road dust chemical profiles for source identification and  
 945 human health impact assessment, *Sci. Rep.*, 10, 14259, 10.1038/s41598-020-71180-x, 2020.  
 946  
 947 Kolattukudy, P. E.: Chemistry and biochemistry of natural waxes, Elsevier Scientific Pub. Co., 1976.  
 948  
 949 Laing, J. R., Hopke, P. K., Hopke, E. F., Husain, L., Dutkiewicz, V. A., Paatero, J., and Viisanen, Y.:  
 950 Positive Matrix Factorization of 47 Years of Particle Measurements in Finnish Arctic, *Aerosol. Air*  
 951 *Qual. Res.*, 15, 188-207 2015.  
 952  
 953 Le, T., Wang, Y., Liu, L., Yang, J., Yung, Y. L., Li, G., and Seinfeld, J. H.: Unexpected air pollution  
 954 with marked emission reductions during the COVID-19 outbreak in China, *Science*, 369, 702,  
 955 10.1126/science.abb7431, 2020.  
 956  
 957 Lee, B.-K., Hieu, N. T. J. A., and Resarch, A. Q.: Seasonal variation and sources of heavy metals in  
 958 atmospheric aerosols in a residential area of Ulsan, Korea, 11, 679-688, 2011.  
 959  
 960 Lee, S., Liu, W., Wang, Y., Russell, A. G., and Edgerton, E. S.: Source apportionment of PM 2.5:  
 961 Comparing PMF and CMB results for four ambient monitoring sites in the southeastern United States,  
 962 *Atmos. Environ.*, 42, 4126-4137, 2008a.  
 963  
 964 Lee, S., Kim, H. K., Yan, B., Cobb, C. E., Hennigan, C., Nichols, S., Chamber, M., Edgerton, E. S.,  
 965 Jansen, J. J., Hu, Y., Zheng, M., Weber, R. J., and Russell, A. G.: Diagnosis of Aged Prescribed  
 966 Burning Plumes Impacting an Urban Area, *Environ. Sci. Technol.*, 42, 1438-1444,  
 967 10.1021/es7023059, 2008b.  
 968

969 Li, M., Liu, Z., Chen, J., Huang, X., Liu, J., Xie, Y., Hu, B., Xu, Z., Zhang, Y., and Wang, Y.:  
 970 Characteristics and source apportionment of metallic elements in PM<sub>2.5</sub> at urban and suburban sites  
 971 in Beijing: Implication of emission reduction, 10, 105, 2019.  
 972  
 973 Li, D., Liu, J., Zhang, J., Gui, H., Du, P., Yu, T., Wang, J., Lu, Y., Liu, W., and Cheng, Y.:  
 974 Identification of long-range transport pathways and potential sources of PM(2.5) and PM(10) in  
 975 Beijing from 2014 to 2015, *J. Environ. Sci. (China)*, 56, 214-229, 10.1016/j.jes.2016.06.035, 2017.  
 976  
 977 Lim, J.-M., Lee, J.-H., Moon, J.-H., Chung, Y.-S., and Kim, K.-H.: Source apportionment of PM<sub>10</sub> at  
 978 a small industrial area using Positive Matrix Factorization, *Atmos. Res.*, 95, 88-100,  
 979 <https://doi.org/10.1016/j.atmosres.2009.08.009>, 2010.  
 980  
 981 Liu, Y., Zheng, M., Yu, M., Cai, X., Du, H., Li, J., Zhou, T., Yan, C., Wang, X., Shi, Z., Harrison, R.  
 982 M., Zhang, Q., and He, K.: High-time-resolution source apportionment of PM<sub>2.5</sub> in Beijing with  
 983 multiple models, *Atmos. Chem. Phys.*, 19, 6595-6609, 10.5194/acp-19-6595-2019, 2019.  
 984  
 985 Lu, X., Yuan, D., Chen, Y., and Fung, J. C. H.: Impacts of urbanization and long-term meteorological  
 986 variations on global PM<sub>2.5</sub> and its associated health burden, *Environ. Pollut.*, 270, 116003,  
 987 <https://doi.org/10.1016/j.envpol.2020.116003>, 2021.  
 988  
 989 Ma, Q., Wu, Y., Tao, J., Xia, Y., Liu, X., Zhang, D., Han, Z., Zhang, X., and Zhang, R.: Variations  
 990 of Chemical composition and source apportionment of PM<sub>2.5</sub> during winter haze episodes in Beijing,  
 991 *Aerosol. Air Qual. Res.*, 17, 2791-2803, 10.4209/aaqr.2017.10.0366, 2017a.  
 992  
 993 Ma, Q., Wu, Y., Zhang, D., Wang, X., Xia, Y., Liu, X., Tian, P., Han, Z., Xia, X., Wang, Y., and  
 994 Zhang, R.: Roles of regional transport and heterogeneous reactions in the PM<sub>2.5</sub> increase during winter  
 995 haze episodes in Beijing, *Sci. Tot. Environ.*, 599-600, 246-253,  
 996 <https://doi.org/10.1016/j.scitotenv.2017.04.193>, 2017b.  
 997  
 998 Mazzei, F., D'Alessandro, A., Lucarelli, F., Nava, S., Prati, P., Valli, G., and Vecchi, R.:  
 999 Characterization of particulate matter sources in an urban environment, *Sci. Tot. Environ.*, 401, 81-  
 1000 89, <https://doi.org/10.1016/j.scitotenv.2008.03.008>, 2008.  
 1001  
 1002 Niu, H., Hu, W., Zhang, D., Wu, Z., Guo, S., Pian, W., Cheng, W., and Hu, M.: Variations of fine  
 1003 particle physiochemical properties during a heavy haze episode in the winter of Beijing, *Sci. Tot.*  
 1004 *Environ.*, 571, 103-109, <https://doi.org/10.1016/j.scitotenv.2016.07.147>, 2016.  
 1005  
 1006 Norris, G., Duvall, R., Brown, S., and Bai, S.: EPA Positive Matrix Factorization (PMF) 5.0  
 1007 fundamentals and User Guide Prepared for the US Environmental Protection Agency Office of  
 1008 Research and Development, Washington, DC, DC EPA/600/R-14/108, 2014.  
 1009  
 1010 Oros, D. R., and Simoneit, B. R. T.: Identification and emission rates of molecular tracers in coal  
 1011 smoke particulate matter, *Fuel*, 79, 515-536, [https://doi.org/10.1016/S0016-2361\(99\)00153-2](https://doi.org/10.1016/S0016-2361(99)00153-2), 2000.  
 1012  
 1013 Paatero, P., and Hopke, P. K.: Discarding or downweighting high-noise variables in factor analytic  
 1014 models, *Anal. Chim. Acta*, 490, 277-289, 2003.  
 1015  
 1016 Paatero, P.: Least squares formulation of robust non-negative factor analysis, *Chemom. Intell. Lab.*  
 1017 *Syst.*, 37, 23-35, [http://doi.org/10.1016/S0169-7439\(96\)00044-5](http://doi.org/10.1016/S0169-7439(96)00044-5), 1997.  
 1018  
 1019 Paatero, P., and Tapper, U.: Positive matrix factorization: A non-negative factor model with optimal  
 1020 utilization of error estimates of data values, *Environmetrics*, 5, 111-126, 1994.

1021 Pant, P., Shukla, A., Kohl, S. D., Chow, J. C., Watson, J. G., and Harrison, R. M.: Characterization  
 1022 of ambient PM<sub>2.5</sub> at a pollution hotspot in New Delhi, India and inference of sources, *Atmos.*  
 1023 *Environ.*, 109, 178-189, <http://dx.doi.org/10.1016/j.atmosenv.2015.02.074>, 2015.

1024  
 1025 Pant, P., and Harrison, R. M.: Estimation of the contribution of road traffic emissions to particulate  
 1026 matter concentrations from field measurements: A review, *Atmos. Environ.*, 77, 78-97,  
 1027 <https://doi.org/10.1016/j.atmosenv.2013.04.028>, 2013.

1028  
 1029 Pant, P., and Harrison, R. M.: Critical review of receptor modelling for particulate matter: a case  
 1030 study of India, *Atmos. Environ.*, 49, 1-12, 2012.

1031  
 1032 Paraskevopoulou, D., Liakakou, E., Gerasopoulos, E., Theodosi, C., and Mihalopoulos, N.: Long-  
 1033 term characterization of organic and elemental carbon in the PM<sub>2.5</sub> fraction: the case of Athens,  
 1034 Greece, *Atmos. Chem. Phys.*, 14, 13313-13325, 10.5194/acp-14-13313-2014, 2014.

1035  
 1036 Paulot, F., Paynter, D., Ginoux, P., Naik, V., Whitburn, S., Van Damme, M., Clarisse, L., Coheur, P.-  
 1037 F., and Horowitz, L. W.: Gas-aerosol partitioning of ammonia in biomass burning plumes:  
 1038 Implications for the interpretation of spaceborne observations of ammonia and the radiative forcing  
 1039 of ammonium nitrate, 44, 8084-8093, <https://doi.org/10.1002/2017GL074215>, 2017.

1040  
 1041 Petit, J. E., Favez, O., Albinet, A., and Canonaco, F.: A user-friendly tool for comprehensive  
 1042 evaluation of the geographical origins of atmospheric pollution: Wind and trajectory analyses,  
 1043 *Environ. Modell. Softw.*, 88, 183-187, <https://doi.org/10.1016/j.envsoft.2016.11.022>, 2017.

1044  
 1045 Piscitello, A., Bianco, C., Casasso, A., and Sethi, R.: Non-exhaust traffic emissions: Sources,  
 1046 characterization, and mitigation measures, *Sci. Total Environ.*, 766, 144440,  
 1047 <https://doi.org/10.1016/j.scitotenv.2020.144440>, 2021.

1048  
 1049 Polissar, A. V., Hopke, P. K., and Poirot, R. L.: Atmospheric aerosol over Vermont: chemical  
 1050 composition and sources, *Environ. Sci. Technol.*, 35, 4604-4621, 2001.

1051  
 1052 Polissar, A. V., Hopke, P. K., Paatero, P., Malm, W. C., and Sisler, J. F.: Atmospheric aerosol over  
 1053 Alaska: 2. Elemental composition and sources, *J. Geophys. Res.-Atmos.*, 103, 19045-19057, 1998.

1054  
 1055 Qiu, Y., Xie, Q., Wang, J., Xu, W., Li, L., Wang, Q., Zhao, J., Chen, Y., Chen, Y., Wu, Y., Du, W.,  
 1056 Zhou, W., Lee, J., Zhao, C., Ge, X., Fu, P., Wang, Z., Worsnop, D. R., and Sun, Y.: Vertical  
 1057 Characterization and Source Apportionment of Water-Soluble Organic Aerosol with High-resolution  
 1058 Aerosol Mass Spectrometry in Beijing, China, *ACS Earth Space Chem.*, 3, 273-284,  
 1059 10.1021/acsearthspacechem.8b00155, 2019.

1060  
 1061 Querol, X., Zhuang, X., Alastuey, A., Viana, M., Lv, W., Wang, Y., López, A., Zhu, Z., Wei, H., and  
 1062 Xu, S.: Speciation and sources of atmospheric aerosols in a highly industrialised emerging mega-city  
 1063 in Central China, *J. Environ. Monit.*, 8, 1049-1059, 10.1039/B608768J, 2006.

1064  
 1065 Rogge, W. F., Hildemann, L. M., Mazurek, M. A., Cass, G. R., and Simoneit, B. R. T.: Sources of  
 1066 fine organic aerosol. 4. Particulate abrasion products from leaf surfaces of urban plants, *Environ. Sci.*  
 1067 *Technol.*, 27, 2700-2711, 10.1021/es00049a008, 1993.

1068  
 1069 Schembari, C., Bove, M. C., Cuccia, E., Cavalli, F., Hjorth, J., Massabò, D., Nava, S., Udisti, R., and  
 1070 Prati, P.: Source apportionment of PM<sub>10</sub> in the Western Mediterranean based on observations from a  
 1071 cruise ship, *Atmos. Environ.*, 98, 510-518, 10.1016/j.atmosenv.2014.09.015, 2014.



1072 Shi, Z., Song, C., Liu, B., Lu, G., Xu, J., Van Vu, T., Elliott, R. J. R., Li, W., Bloss, W. J., and  
1073 Harrison, R. M.: Abrupt but smaller than expected changes in surface air quality attributable to  
1074 COVID-19 lockdowns, *Sci. Adv.*, 7, 10.1126/sciadv.abd6696, 2021.

1075  
1076 Shi, Z., Vu, T., Kotthaus, S., Harrison, R. M., Grimmond, S., Yue, S., Zhu, T., Lee, J., Han, Y.,  
1077 Demuzere, M., Dunmore, R. E., Ren, L., Liu, D., Wang, Y., Wild, O., Allan, J., Acton, W. J., Barlow,  
1078 J., Barratt, B., Beddows, D., Bloss, W. J., Calzolari, G., Carruthers, D., Carslaw, D. C., Chan, Q.,  
1079 Chatzidiakou, L., Chen, Y., Crilley, L., Coe, H., Dai, T., Doherty, R., Duan, F., Fu, P., Ge, B., Ge,  
1080 M., Guan, D., Hamilton, J. F., He, K., Heal, M., Heard, D., Hewitt, C. N., Hollaway, M., Hu, M., Ji,  
1081 D., Jiang, X., Jones, R., Kalberer, M., Kelly, F. J., Kramer, L., Langford, B., Lin, C., Lewis, A. C.,  
1082 Li, J., Li, W., Liu, H., Liu, J., Loh, M., Lu, K., Lucarelli, F., Mann, G., McFiggans, G., Miller, M. R.,  
1083 Mills, G., Monk, P., Nemitz, E., O'Connor, F., Ouyang, B., Palmer, P. I., Percival, C., Popoola, O.,  
1084 Reeves, C., Rickard, A. R., Shao, L., Shi, G., Spracklen, D., Stevenson, D., Sun, Y., Sun, Z., Tao, S.,  
1085 Tong, S., Wang, Q., Wang, W., Wang, X., Wang, X., Wang, Z., Wei, L., Whalley, L., Wu, X., Wu,  
1086 Z., Xie, P., Yang, F., Zhang, Q., Zhang, Y., Zhang, Y., and Zheng, M.: Introduction to the special  
1087 issue "In-depth study of air pollution sources and processes within Beijing and its surrounding region  
1088 (APHH-Beijing)", *Atmos. Chem. Phys.*, 19, 7519-7546, 10.5194/acp-19-7519-2019, 2019.

1089  
1090 Shrivastava, M. K., Subramanian, R., Rogge, W. F., and Robinson, A. L.: Sources of organic aerosol:  
1091 Positive matrix factorization of molecular marker data and comparison of results from different  
1092 source apportionment models, *Atmos. Environ.*, 41, 9353-9369, 10.1016/j.atmosenv.2007.09.016,  
1093 2007.

1094  
1095 Simoneit, B. R.: A review of biomarker compounds as source indicators and tracers for air pollution,  
1096 *Environ. Sci. Pollut. Res.*, 6, 159-169, 1999.

1097  
1098 Smichowski, P., Gómez, D., Frazzoli, C., and Caroli, S.: Traffic-Related Elements in Airborne  
1099 Particulate Matter, *Applied Spectroscopy Reviews*, 43, 23-49, 10.1080/05704920701645886, 2007.

1100  
1101 Song, Y., Tang, X., Xie, S., Zhang, Y., Wei, Y., Zhang, M., Zeng, L., and Lu, S.: Source  
1102 apportionment of PM<sub>2.5</sub> in Beijing in 2004, *J. Hazard. Mater.*, 146, 124-130,  
1103 <https://doi.org/10.1016/j.jhazmat.2006.11.058>, 2007.

1104  
1105 Song, Y., Zhang, Y., Xie, S., Zeng, L., Zheng, M., Salmon, L. G., Shao, M., and Slanina, S.: Source  
1106 apportionment of PM<sub>2.5</sub> in Beijing by positive matrix factorization, *Atmos. Environ.*, 40, 1526-1537,  
1107 10.1016/j.atmosenv.2005.10.039, 2006.

1108  
1109 Sörme, L., Bergbäck, B., and Lohm, U.: Goods in the Anthroposphere as a Metal Emission Source A  
1110 Case Study of Stockholm, Sweden, *Water, Air & Soil Pollut.: Focus*, 1, 213-227,  
1111 10.1023/A:1017516523915, 2001.

1112  
1113 Srimuruganandam, B., and Shiva Nagendra, S. M.: Application of positive matrix factorization in  
1114 characterization of PM<sub>10</sub> and PM<sub>2.5</sub> emission sources at urban roadside, *Chemosphere*, 88, 120-130,  
1115 <http://doi.org/10.1016/j.chemosphere.2012.02.083>, 2012.

1116  
1117 Srivastava, D., Tomaz, S., Favez, O., Lanzafame, G. M., Golly, B., Besombes, J. L., Alleman, L. Y.,  
1118 Jaffrezo, J. L., Jacob, V., Perraudin, E., Villenave, E., and Albinet, A.: Speciation of organic fraction  
1119 does matter for source apportionment. Part 1: A one-year campaign in Grenoble (France), *Sci. Tot.*  
1120 *Environ.*, 624, 1598-1611, 10.1016/j.scitotenv.2017.12.135, 2018.

1121

1122 Stein, A. F., Draxler, R. R., Rolph, G. D., Stunder, B. J. B., Cohen, M. D., and Ngan, F.: NOAA's  
 1123 HYSPLIT Atmospheric Transport and Dispersion Modeling System, *Bull. Am. Meteorol. Soc.*, 96,  
 1124 2059-2077, 10.1175/bams-d-14-00110.1, 2015.

1125

1126 Sun, Y., He, Y., Kuang, Y., Xu, W., Song, S., Ma, N., Tao, J., Cheng, P., Wu, C., Su, H., Cheng, Y.,  
 1127 Xie, C., Chen, C., Lei, L., Qiu, Y., Fu, P., Croteau, P., and Worsnop, D. R.: Chemical differences  
 1128 between PM<sub>1</sub> and PM<sub>2.5</sub> in Highly polluted environment and implications in air pollution studies,  
 1129 *Geophys. Res. Lett.*, 47, e2019GL086288, 10.1029/2019GL086288, 2020.

1130

1131 Sun, Y., Du, W., Fu, P., Wang, Q., Li, J., Ge, X., Zhang, Q., Zhu, C., Ren, L., Xu, W., Zhao, J., Han,  
 1132 T., Worsnop, D. R., and Wang, Z.: Primary and secondary aerosols in Beijing in winter: sources,  
 1133 variations and processes, *Atmos. Chem. Phys.*, 16, 8309-8329, 10.5194/acp-16-8309-2016, 2016.

1134

1135 Sun, Y., Jiang, Q., Wang, Z., Fu, P., Li, J., Yang, T., and Yin, Y.: Investigation of the sources and  
 1136 evolution processes of severe haze pollution in Beijing in January 2013, 119, 4380-4398,  
 1137 <https://doi.org/10.1002/2014JD021641>, 2014.

1138

1139 Sun, Y. L., Wang, Z. F., Fu, P. Q., Yang, T., Jiang, Q., Dong, H. B., Li, J., and Jia, J. J.: Aerosol  
 1140 composition, sources and processes during wintertime in Beijing, China, *Atmos. Chem. Phys.*, 13,  
 1141 4577-4592, 10.5194/acp-13-4577-2013, 2013.

1142

1143 Sun, J., Zhang, Q., Canagaratna, M. R., Zhang, Y., Ng, N. L., Sun, Y., Jayne, J. T., Zhang, X., Zhang,  
 1144 X., and Worsnop, D. R.: Highly time- and size-resolved characterization of submicron aerosol  
 1145 particles in Beijing using an Aerodyne Aerosol Mass Spectrometer, *Atmos. Environ.*, 44, 131-140,  
 1146 <https://doi.org/10.1016/j.atmosenv.2009.03.020>, 2010.

1147

1148 Sun, Y., Zhuang, G., Tang, A., Wang, Y., and An, Z.: Chemical Characteristics of PM<sub>2.5</sub> and PM<sub>10</sub>  
 1149 in Haze–Fog Episodes in Beijing, *Environ. Sci. Technol.*, 40, 3148-3155, 10.1021/es051533g, 2006.

1150

1151 Sun, Y., Zhuang, G., Wang, Y., Zhao, X., Li, J., Wang, Z., and An, Z.: Chemical composition of dust  
 1152 storms in Beijing and implications for the mixing of mineral aerosol with pollution aerosol on the  
 1153 pathway, *J. Geophys. Chem.*, 110, D24209, 10.1029/2005jd006054, 2005.

1154

1155 Swietlicki, E., and Krejci, R.: Source characterisation of the Central European atmospheric aerosol  
 1156 using multivariate statistical methods, *Nucl. Instrum. Methods Phys. Res., Sect. B*, 109-110, 519-525,  
 1157 [https://doi.org/10.1016/0168-583X\(95\)01220-6](https://doi.org/10.1016/0168-583X(95)01220-6), 1996.

1158

1159 Takuwa, T., Mkilaha, I. S. N., and Naruse, I.: Mechanisms of fine particulates formation with alkali  
 1160 metal compounds during coal combustion, *Fuel*, 85, 671–678, 2006.

1161

1162 Tao, S., Ru, M. Y., Du, W., Zhu, X., Zhong, Q. R., Li, B. G., Shen, G. F., Pan, X. L., Meng, W. J.,  
 1163 Chen, Y. L., Shen, H. Z., Lin, N., Su, S., Zhuo, S. J., Huang, T. B., Xu, Y., Yun, X., Liu, J. F., Wang,  
 1164 X. L., Liu, W. X., Chen, H. F., and Zhu, D. Q.: Quantifying the Rural Residential Energy Transition  
 1165 in China from 1992 to 2012 through a Representative National Survey, *Nat. Energy*, 3, 567–573,  
 1166 2018.

1167

1168 Thorpe, A., and Harrison, R. M.: Sources and properties of non-exhaust particulate matter from road  
 1169 traffic: A review, *Sci. Tot. Environ.*, 400, 270-282, <https://doi.org/10.1016/j.scitotenv.2008.06.007>,  
 1170 2008.

1171

1172 Tian, S. L., Pan, Y. P., and Wang, Y. S.: Size-resolved source apportionment of particulate matter in  
 1173 urban Beijing during haze and non-haze episodes, *Atmos. Chem. Phys.*, 16, 1-19, 10.5194/acp-16-1-  
 1174 2016, 2016.

1175

1176 Tie, X., Huang, R.-J., Cao, J., Zhang, Q., Cheng, Y., Su, H., Chang, D., Pöschl, U., Hoffmann, T.,  
 1177 Dusek, U., Li, G., Worsnop, D. R., and O'Dowd, C. D.: Severe Pollution in China Amplified by  
 1178 Atmospheric Moisture, *Sci. Rep.*, 7, 15760-15760, 10.1038/s41598-017-15909-1, 2017.

1179

1180 Vejehati, F., Xu, Z., and Gupta, R.: Trace elements in coal: Associations with coal and minerals and  
 1181 their behavior during coal utilization – A review, *Fuel*, 89, 904-911,  
 1182 <https://doi.org/10.1016/j.fuel.2009.06.013>, 2010.

1183

1184 Viana, M., Kuhlbusch, T. A. J., Querol, X., Alastuey, A., Harrison, R. M., Hopke, P. K., Winiwarter,  
 1185 W., Vallius, M., Szidat, S., Prévôt, A. S. H., Hueglin, C., Bloemen, H., Wählin, P., Vecchi, R.,  
 1186 Miranda, A. I., Kasper-Giebl, A., Maenhaut, W., and Hitzenberger, R.: Source apportionment of  
 1187 particulate matter in Europe: A review of methods and results, *J. Aerosol Sci.*, 39, 827-849,  
 1188 <http://dx.doi.org/10.1016/j.jaerosci.2008.05.007>, 2008.

1189

1190 Vu, T. V., Shi, Z., Cheng, J., Zhang, Q., He, K., Wang, S., and Harrison, R. M.: Assessing the impact  
 1191 of clean air action on air quality trends in Beijing using a machine learning technique, *Atmos. Chem.*  
 1192 *Phys.*, 19, 11303-11314, 10.5194/acp-19-11303-2019, 2019.

1193

1194 Waked, A., Favez, O., Alleman, L. Y., Piot, C., Petit, J. E., Delaunay, T., Verlinden, E., Golly, B.,  
 1195 Besombes, J. L., Jaffrezo, J. L., and Leoz-Garziandia, E.: Source apportionment of PM<sub>10</sub> in a north-  
 1196 western Europe regional urban background site (Lens, France) using positive matrix factorization and  
 1197 including primary biogenic emissions, *Atmos. Chem. Phys.*, 14, 3325-3346, 10.5194/acp-14-3325-  
 1198 2014, 2014.

1199

1200 Wang, G., Gu, S., Chen, J., Wu, X., and Yu, J.: Assessment of health and economic effects by PM<sub>2.5</sub>  
 1201 pollution in Beijing: a combined exposure–response and computable general equilibrium analysis,  
 1202 *Environ. Technol.*, 37, 3131-3138, 10.1080/09593330.2016.1178332, 2016.

1203

1204 Wang, L., Zhang, N., Liu, Z., Sun, Y., Ji, D., and Wang, Y.: The Influence of Climate Factors,  
 1205 Meteorological Conditions, and boundary-layer structure on severe haze pollution in the Beijing-  
 1206 Tianjin-Hebei region during January 2013, *Adv. Meteorol.*, 2014, 685971, 10.1155/2014/685971,  
 1207 2014.

1208

1209 Wang, Y., Hopke, P. K., Xia, X., Rattigan, O. V., Chalupa, D. C., and Utell, M. J.: Source  
 1210 apportionment of airborne particulate matter using inorganic and organic species as tracers, *Atmos.*  
 1211 *Environ.*, 55, 525-532, 2012.

1212

1213 Wang, Q., Shao, M., Zhang, Y., Wei, Y., Hu, M., and Guo, S.: Source apportionment of fine organic  
 1214 aerosols in Beijing, *Atmos. Chem. Phys.*, 9, 8573-8585, 10.5194/acp-9-8573-2009, 2009.

1215

1216 Wang, H., Zhuang, Y., Wang, Y., Sun, Y., Yuan, H., Zhuang, G., and Hao, Z.: Long-term monitoring  
 1217 and source apportionment of PM<sub>2.5</sub>/PM<sub>10</sub> in Beijing, China, *J. Environ. Sci.*, 20, 1323-1327,  
 1218 [https://doi.org/10.1016/S1001-0742\(08\)62228-7](https://doi.org/10.1016/S1001-0742(08)62228-7), 2008.

1219

1220 Watson, J. G., Robinson, N. F., Chow, J. C., Henry, R. C., Kim, B., Pace, T., Meyer, E. L., and  
 1221 Nguyen, Q.: The USEPA/DRI chemical mass balance receptor model, CMB 7.0, *Environ. Soft.*, 5,  
 1222 38-49, 1990.



1223  
1224 Wu, X., Chen, C., Vu, T. V., Liu, D., Baldo, C., Shen, X., Zhang, Q., Cen, K., Zheng, M., He, K.,  
1225 Shi, Z., and Harrison, R. M.: Source apportionment of fine organic carbon (OC) using receptor  
1226 modelling at a rural site of Beijing: Insight into seasonal and diurnal variation of source contributions,  
1227 *Environ. Pollut.*, 115078, 2020.

1228  
1229 Wu, P., Ding, Y., and Liu, Y. J. A. i. A. S.: Atmospheric circulation and dynamic mechanism for  
1230 persistent haze events in the Beijing–Tianjin–Hebei region, *Adv. Atmos. Sci.*, 34, 429-440, 2017.

1231  
1232 Xie, Y., Dai, H., Zhang, Y., Wu, Y., Hanaoka, T., and Masui, T. J. E. i.: Comparison of health and  
1233 economic impacts of PM<sub>2.5</sub> and ozone pollution in China, *Environ. Int.*, 130, 104881,  
1234 <https://doi.org/10.1016/j.envint.2019.05.075>, 2019.

1235  
1236 Xing, Y.-F., Xu, Y.-H., Shi, M.-H., and Lian, Y.-X.: The impact of PM<sub>2.5</sub> on the human respiratory  
1237 system, *J. Thorac. Dis.*, 8, E69-E74, 10.3978/j.issn.2072-1439.2016.01.19, 2016.

1238  
1239 Xu, J., Liu, D., Wu, X., Vu, T., V.; Zhang, Y., Fu, P., Sun, Y., Harrison, R., M.; and Shi, Z.: Source  
1240 apportionment of fine aerosol at an urban site of Beijing using a chemical mass balance model, *Atmos.*  
1241 *Chem. Phys.*, 7321–7341, <https://doi.org/10.5194/acp-21-7321-2021>, 2021.

1242  
1243 Xu, W., Sun, Y., Wang, Q., Zhao, J., Wang, J., Ge, X., Xie, C., Zhou, W., Du, W., Li, J., Fu, P.,  
1244 Wang, Z., Worsnop, D. R., and Coe, H.: Changes in aerosol chemistry from 2014 to 2016 in winter  
1245 in Beijing: Insights from high-resolution aerosol mass spectrometry, *J. Geophys. Res.-Atmos.*, 124,  
1246 1132-1147, 10.1029/2018JD029245, 2019.

1247  
1248 Yan, C., Zheng, M., Sullivan, A. P., Shen, G., Chen, Y., Wang, S., Zhao, B., Cai, S., Desyaterik, Y.,  
1249 Li, X., Zhou, T., Gustafsson, Ö., and Collett, J. L.: Residential coal combustion as a source of  
1250 levoglucosan in China, *Environ. Sci. Technol.*, 52, 1665-1674, 10.1021/acs.est.7b05858, 2018.

1251  
1252 Yu, L., Wang, G., Zhang, R., Zhang, L., Song, Y., Wu, B., Li, X., An, K., and Chu, J.:  
1253 Characterization and source apportionment of PM<sub>2.5</sub> in an urban environment in Beijing, *Aerosol Air*  
1254 *Qual. Res.*, 13, 574-583, 10.4209/aaqr.2012.07.0192, 2013.

1255  
1256 Zhang, Y., Ren, H., Sun, Y., Cao, F., Chang, Y., Liu, S., Lee, X., Agrios, K., Kawamura, K., Liu, D.,  
1257 Ren, L., Du, W., Wang, Z., Prévôt, A. S. H., Szidat, S., and Fu, P.: High contribution of nonfossil  
1258 sources to submicrometer organic aerosols in Beijing, China, *Environ. Sci. Technol.*, 51, 7842-7852,  
1259 10.1021/acs.est.7b01517, 2017.

1260  
1261 Zhang, J. K., Cheng, M. T., Ji, D. S., Liu, Z. R., Hu, B., Sun, Y., and Wang, Y. S.: Characterization  
1262 of submicron particles during biomass burning and coal combustion periods in Beijing, China, *Sci.*  
1263 *Tot. Environ.*, 562, 812-821, <https://doi.org/10.1016/j.scitotenv.2016.04.015>, 2016.

1264  
1265 Zhang, J.-J., Cui, M.-M., Fan, D., Zhang, D.-S., Lian, H.-X., Yin, Z.-Y., and Li, J.: Relationship  
1266 between haze and acute cardiovascular, cerebrovascular, and respiratory diseases in Beijing,  
1267 *Environ. Sci. Pollut. Res.*, 22, 3920-3925, 10.1007/s11356-014-3644-7, 2015.

1268  
1269 Zhang, J., Wang, Y., Huang, X., Liu, Z., Ji, D., and Sun, Y.: Characterization of organic aerosols in  
1270 Beijing using an aerodyne high-resolution aerosol mass spectrometer, *Adv. Atmos. Sci.*, 32, 877-888,  
1271 10.1007/s00376-014-4153-9, 2015.

1272 Zhang, J. K., Sun, Y., Liu, Z. R., Ji, D. S., Hu, B., Liu, Q., and Wang, Y. S.: Characterization of  
 1273 submicron aerosols during a month of serious pollution in Beijing, 2013, *Atmos. Chem. Phys.*, 14,  
 1274 2887-2903, 10.5194/acp-14-2887-2014, 2014.

1275

1276

1277 Zhang, R., Jing, J., Tao, J., Hsu, S.-C., Wang, G., Cao, J., Lee, C. S. L., Zhu, L., Chen, Z., Zhao, Y.,  
 1278 and Shen, Z.: Chemical characterization and source apportionment of PM<sub>2.5</sub> in Beijing: seasonal  
 1279 perspective, *Atmos. Chem. Phys.*, 13, 7053–7074, <https://doi.org/10.5194/acp-13-7053-2013>, 2013.

1280

1281 Zhang, Q., Jimenez, J. L., Canagaratna, M. R., Ulbrich, I. M., Ng, N. L., Worsnop, D. R., and Sun,  
 1282 Y.: Understanding atmospheric organic aerosols via factor analysis of aerosol mass spectrometry: a  
 1283 review, *Anal. Bioanal. Chem.*, 401, 3045-3067, 2011.

1284

1285 Zhang, X., Hecobian, A., Zheng, M., Frank, N. H., and Weber, R. J.: Biomass burning impact on  
 1286 PM<sub>2.5</sub> over the southeastern US during 2007: integrating chemically speciated FRM filter  
 1287 measurements, MODIS fire counts and PMF analysis, *Atmos. Chem. Phys.*, 10, 6839-6853,  
 1288 10.5194/acp-10-6839-2010, 2010.

1289

1290 Zhang, Y., Sheesley, R. J., Schauer, J. J., Lewandowski, M., Jaoui, M., Offenberger, J. H., Kleindienst,  
 1291 T. E., and Edney, E. O.: Source apportionment of primary and secondary organic aerosols using  
 1292 positive matrix factorization (PMF) of molecular markers, *Atmos. Environ.*, 43, 5567-5574, 2009.

1293

1294 Zhang, Y., Schauer, J. J., Zhang, Y., Zeng, L., Wei, Y., Liu, Y., and Shao, M.: Characteristics of  
 1295 particulate carbon emissions from real-world Chinese coal combustion, *Environ. Sci. Technol.*, 42,  
 1296 5068-5073, 10.1021/es7022576, 2008.

1297

1298 Zhang, Y.-x., Min, S., Zhang, Y.-h., Zeng, L.-m., He, L.-y., Bin, Z., Wei, Y.-j., and Zhu, X.-l.: Source  
 1299 profiles of particulate organic matters emitted from cereal straw burnings, *Journal of Environmental*  
 1300 *Sciences*, 19, 167-175, 2007.

1301

1302 Zhao, Z.-Y., Cao, F., Fan, M.-Y., Zhang, W.-Q., Zhai, X.-Y., Wang, Q., and Zhang, Y.-L. J. A. E.:  
 1303 Coal and biomass burning as major emissions of NO<sub>x</sub> in Northeast China: Implication from dual  
 1304 isotopes analysis of fine nitrate aerosols, *Atmos. Environ.*, 242, 117762, 2020.

1305

1306 Zhao, X., Hu, Q., Wang, X., Ding, X., He, Q., Zhang, Z., Shen, R., Lü, S., Liu, T., Fu, X., and Chen,  
 1307 L.: Composition profiles of organic aerosols from Chinese residential cooking: case study in urban  
 1308 Guangzhou, south China, *J. Atmos. Chem.*, 72, 1-18, 10.1007/s10874-015-9298-0, 2015.

1309

1310 Zheng, M., Salmon, L. G., Schauer, J. J., Zeng, L., Kiang, C. S., Zhang, Y., and Cass, G. R.: Seasonal  
 1311 trends in PM<sub>2.5</sub> source contributions in Beijing, China, *Atmos. Environ.*, 39, 3967-3976,  
 1312 <https://doi.org/10.1016/j.atmosenv.2005.03.036>, 2005.

1313

1314 Zhou, Y., Zheng, N., Luo, L., Zhao, J., Qu, L., Guan, H., Xiao, H., Zhang, Z., Tian, J., and Xiao, H.:  
 1315 Biomass burning related ammonia emissions promoted a self-amplifying loop in the urban  
 1316 environment in Kunming (SW China), *Atmos. Environ.*, 118138,  
 1317 <https://doi.org/10.1016/j.atmosenv.2020.118138>, 2020.

1318 **FIGURE LEGENDS**

1319 **Figure 1.** Factor profiles for identified factors at IAP and PG. The bars show the composition  
1320 profile (left axis) and the dots, the Explained Variation (right axis).

1321 **Figure 2.** Temporal variation of identified factors at IAP and PG. Solid and broken lines represent  
1322 IAP and PG, respectively.

1323 **Figure 3.** Contribution of different sources to PM<sub>2.5</sub> mass at IAP and PG.

1324 **Figure 4.** Correlations observed between PMF and CMB results at IAP. \*If two outlying points  
1325 are removed from the coal combustion-PMF, correlations are markedly improved.

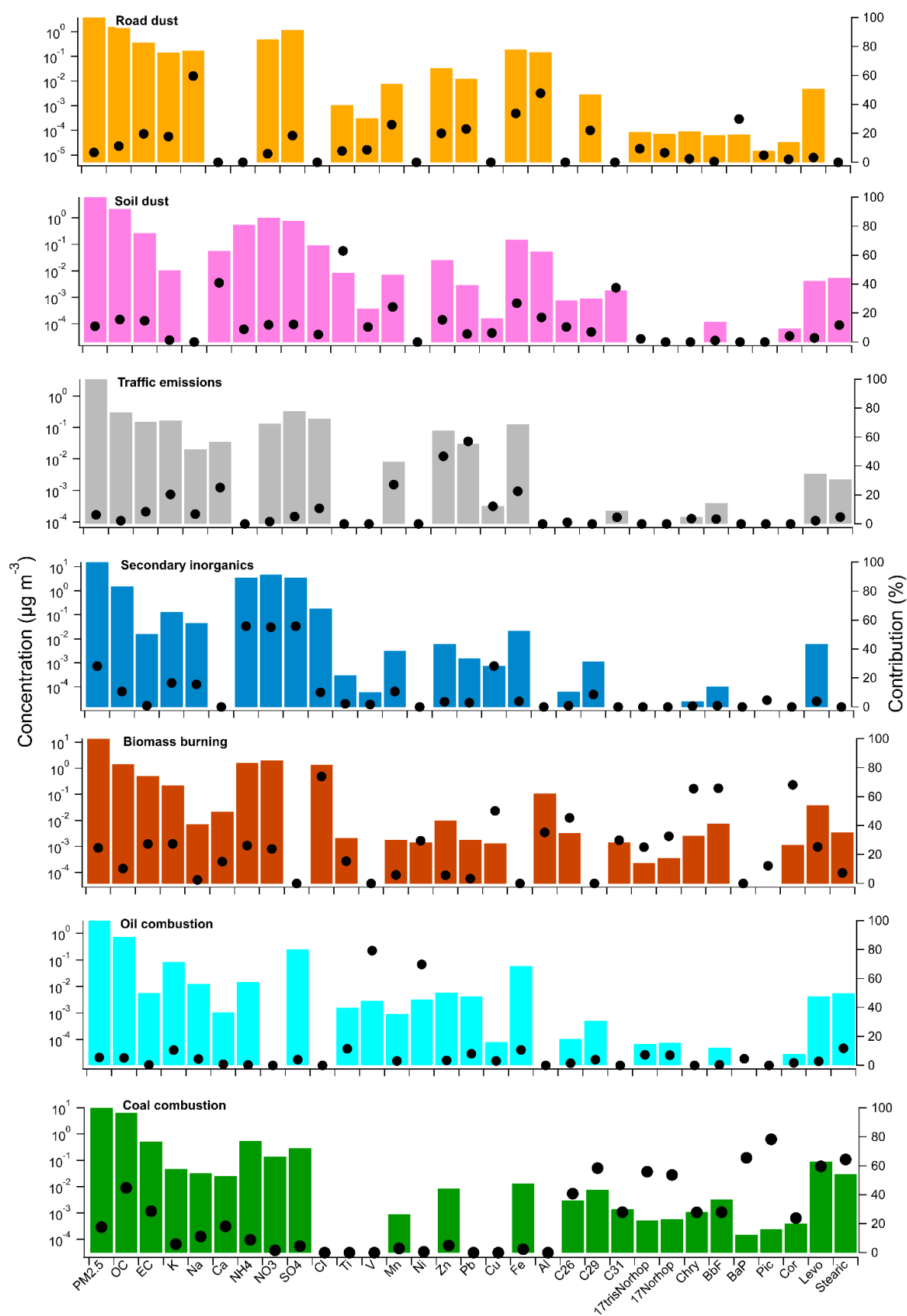
1326 **Figure 5.** Correlations observed between PMF and CMB results at PG.

1327 **Figure 6.** Correlations observed between PMF and online AMS PMF results at IAP (winter). \*If  
1328 two outlying points are removed from the coal combustion-PMF, correlations are  
1329 markedly improved.

1330 **Figure 7.** Correlations observed between PMF and offline AMS PMF results at IAP (winter).

1331

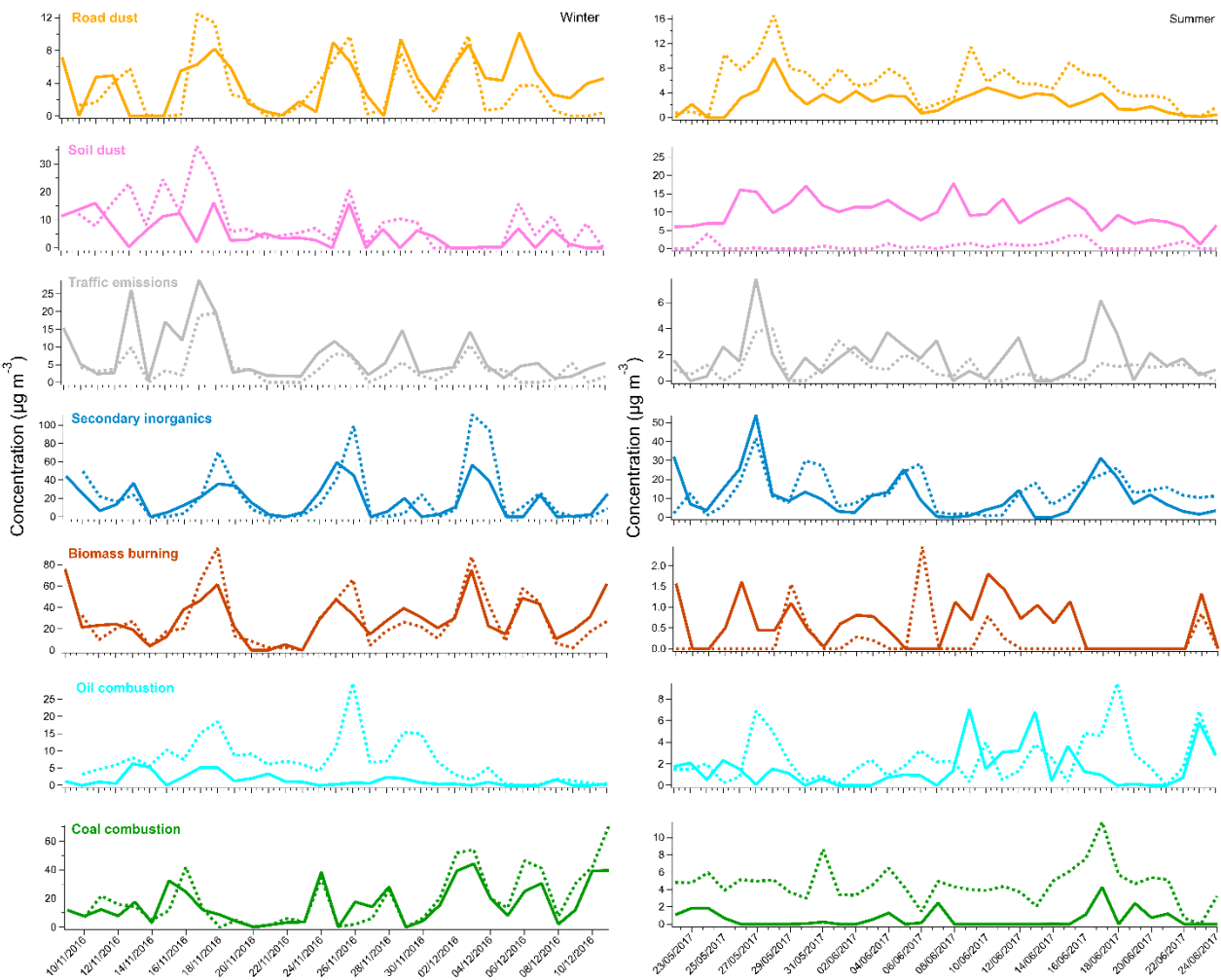
1332



1333

1334 **Figure 1.** Factor profiles for identified factors at IAP and PG. The bars show the composition profile  
 1335 (left axis) and the dots, the Explained Variation (right axis).

1336



1337

1338 **Figure 2.** Temporal variation of identified factors at IAP and PG. Solid and broken lines represent  
1339 IAP and PG, respectively.  
1340

1341

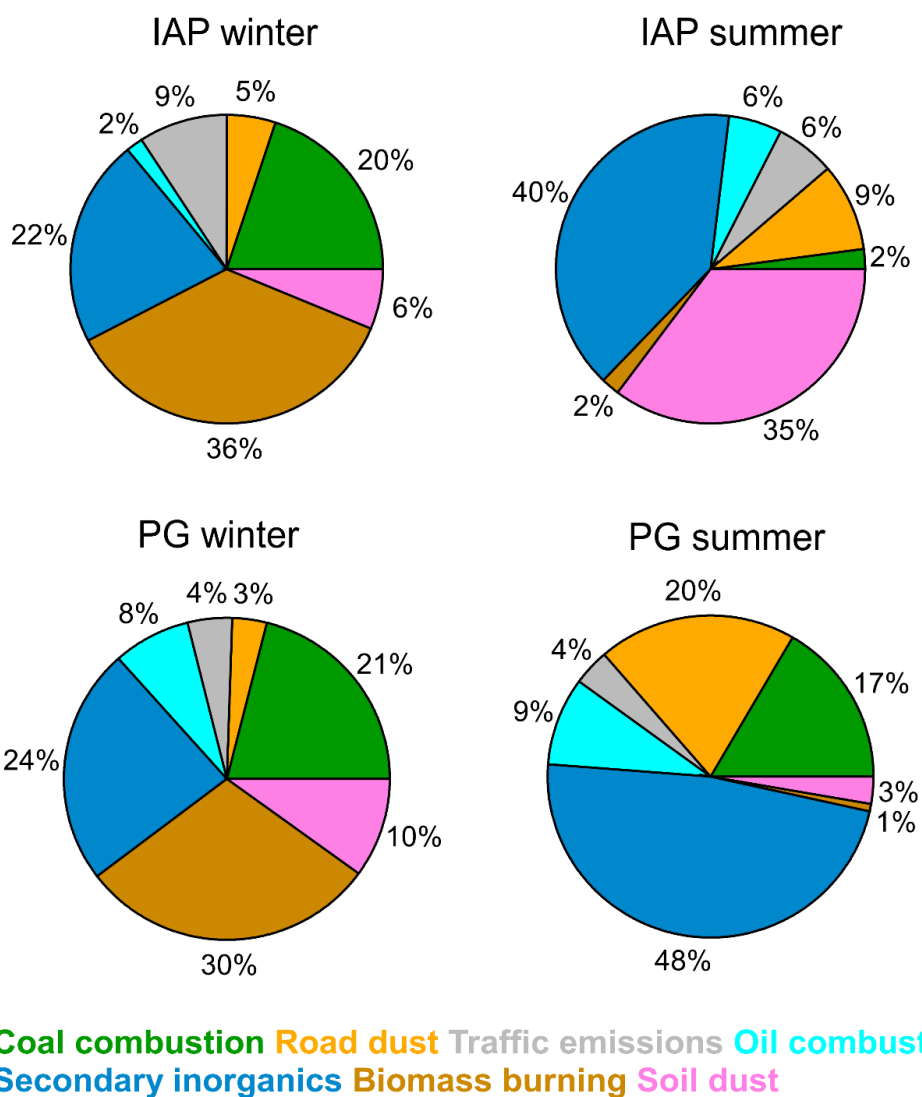
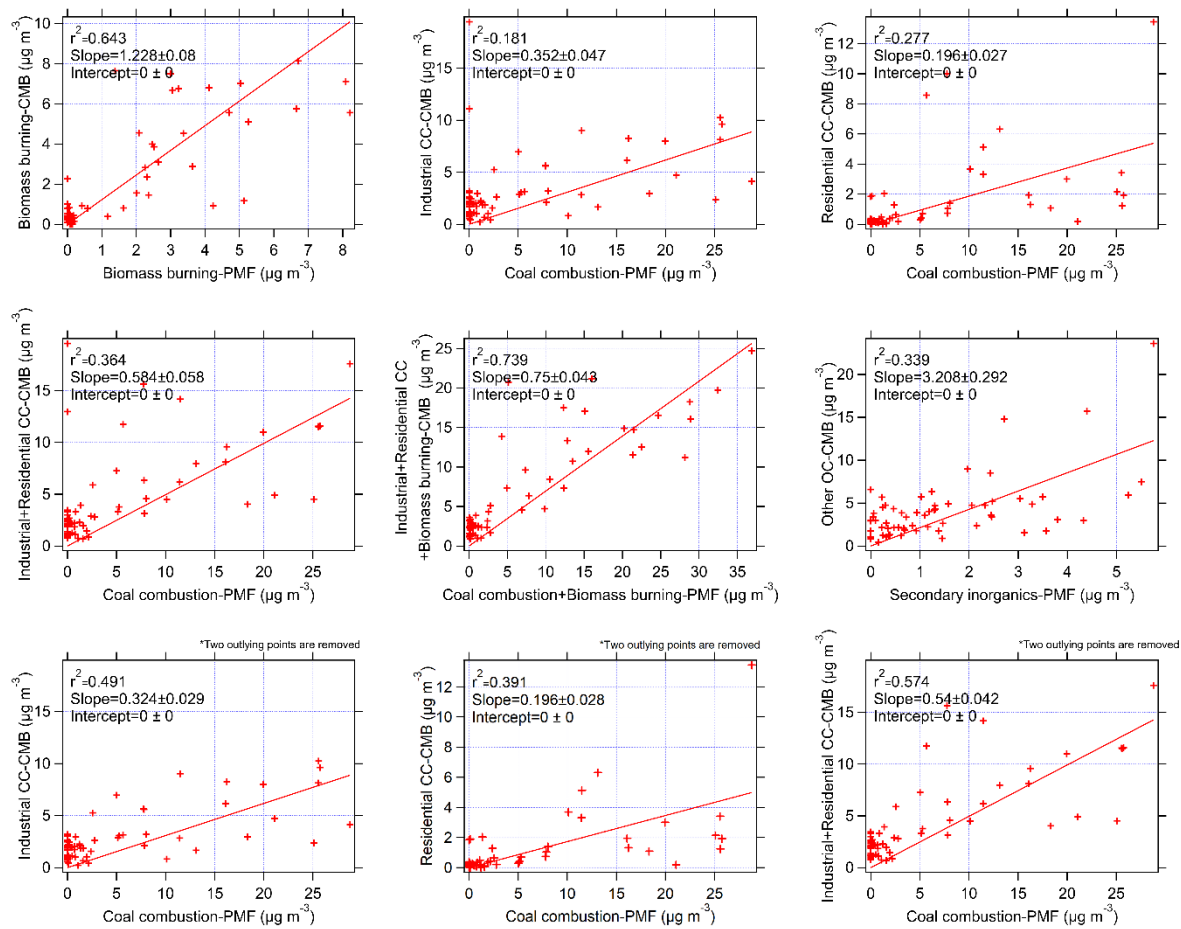


**Figure 3.** Contribution of different sources to PM<sub>2.5</sub> mass at IAP and PG.

1345



1346

1347 **Figure 4.** Correlations observed between PMF and CMB results at IAP. \*If two outlying points are  
1348 removed from the coal combustion-PMF, correlations are markedly improved.

1349

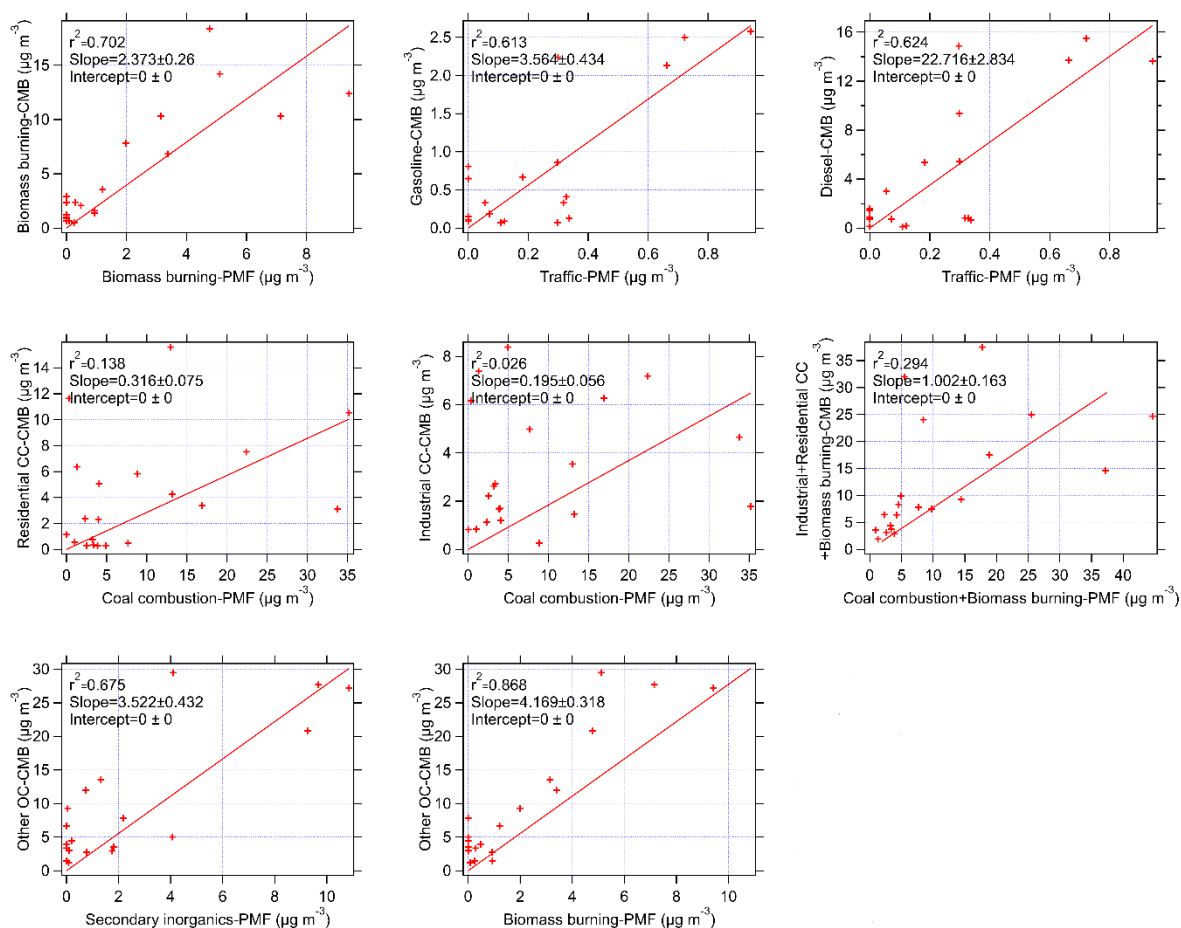


**Figure 5.** Correlations observed between PMF and CMB results at PG.



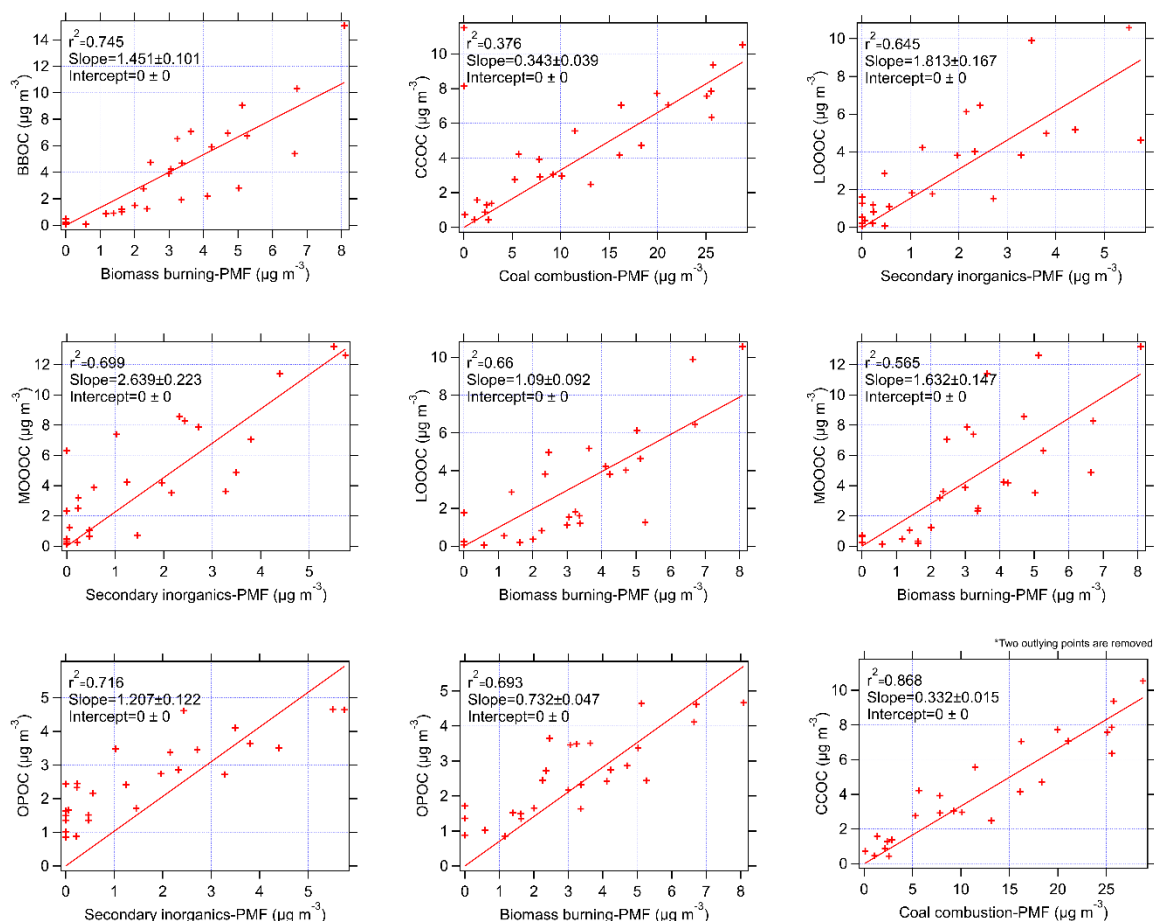
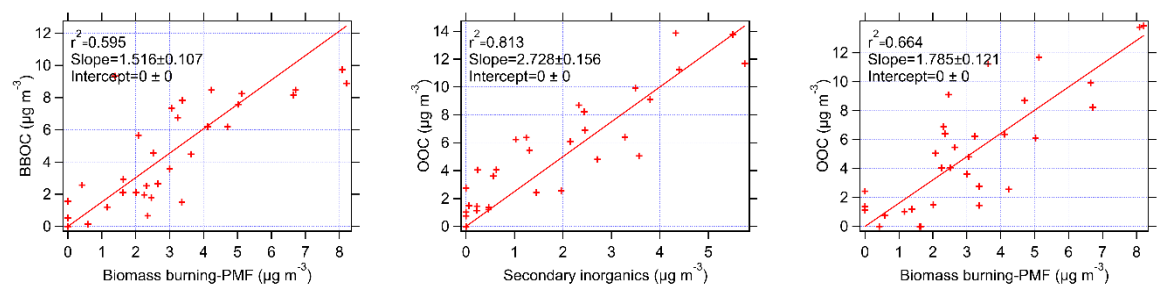


**Figure 6.** Correlations observed between PMF and online AMS PMF results at IAP (winter). \*If two outlying points are removed from the coal combustion-PMF, correlations are markedly improved.

1357



1358

1359 **Figure 7.** Correlations observed between PMF and offline AMS PMF results at IAP (winter).  
1360  
1361